Supporting Information for

Silver complexes with substituted terpyridine as promising anticancer metallodrugs and their crystal structure, photoluminescence, DNA interactions

Jiahe Li, [a,b,c,d] Zhiyuan Wang, [a] Zhongting Chen,[d] Xingyong Xue, [a] Kejuan Lin, [a] Hailan Chen,[e] Lixia Pan,[b] Yulin Yuan*[f] and Zhen Ma*[a,c]

[a] School of Chemistry and Chemical Engineering, Guangxi University, Nanning 530004, People's Republic of China. E-mail: mzmz2009@sohu.com.

[b] National Engineering Research Center for Non-Food Biorefinery, State Key Laboratory of Non-Food Biomass and Enzyme Technology, Guangxi Academy of Sciences, Nanning 530007, People's Republic of China.

[c] Centro de Química Estrutural, Instituto Superior Técnico, Universidade de Lisboa, Av. Rovisco Pais, Lisbon 1049-001, Portugal.

[d] Department of Emergency Medicine, Second Affiliated Hospital of Zhejiang University, Key Laboratory of The Diagnosis and Treatment of Severe Trauma and Burns of Zhejiang Province, Clinical Research Center for Emergency and Critical Care Medicine of Zhejiang Province, Hangzhou 310009, People's Republic of China

[e] School of Animal Science and Technology, Guangxi University, Nanning 530004, People's Republic of China.

[f] Department of Laboratory Medicine, Guangxi Academy of Medical Sciences, The People's Hospital of Guangxi Zhuang Autonomous Region, Nanning 530021, People's Republic of China. E-mail: yuanyulin@126.com.

INDEX

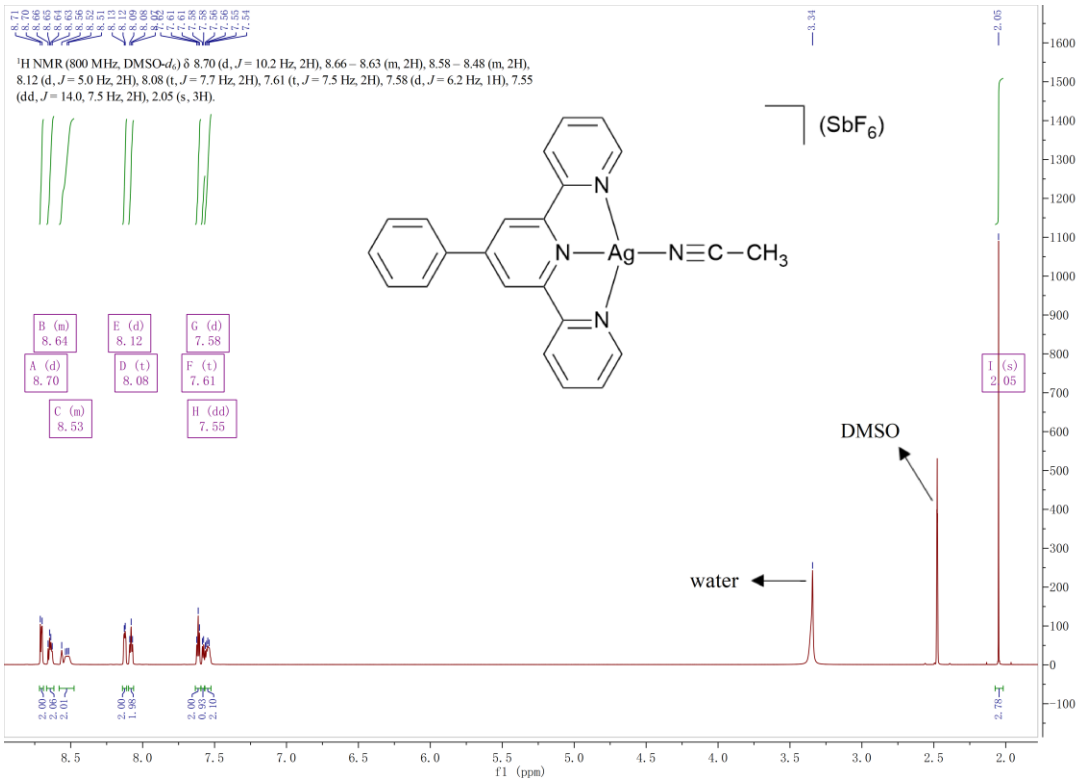

Figure S1 ^{1}H NMR spectrum of compound **1** in DMSO (800 MHz).

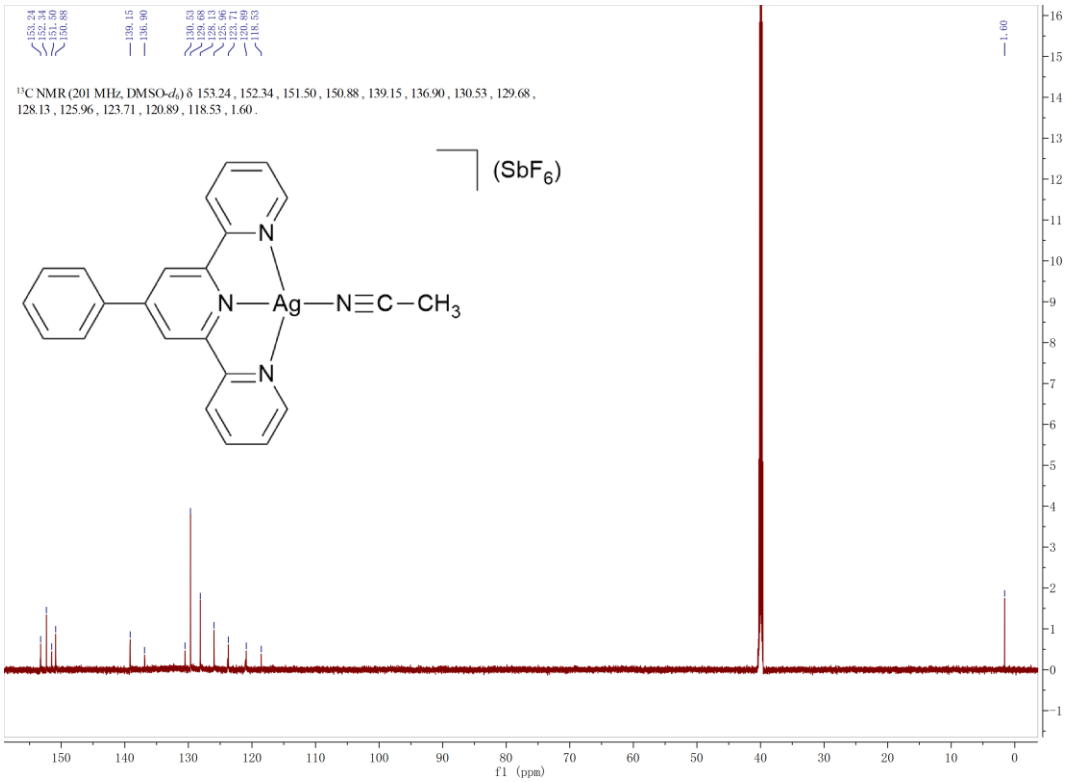

Figure S2 ^{13}C NMR spectrum of compound **1** in DMSO (201 MHz).

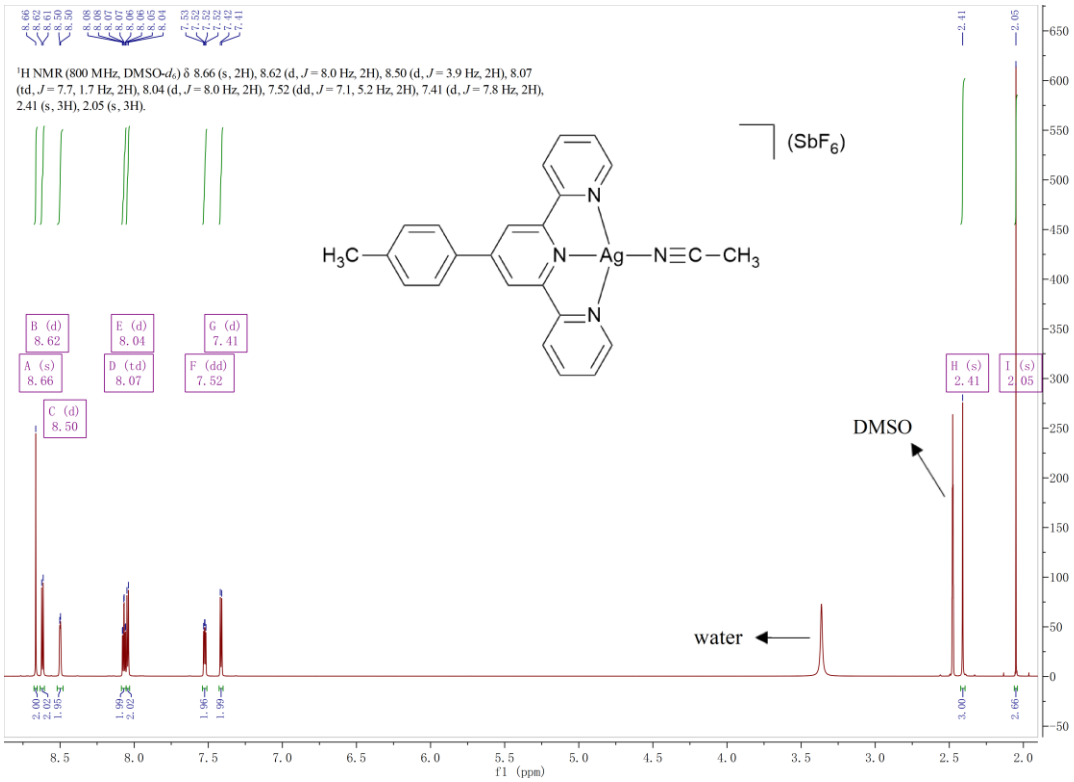

Figure S3 [1]H NMR spectrum of compound **2** in DMSO (800 MHz).

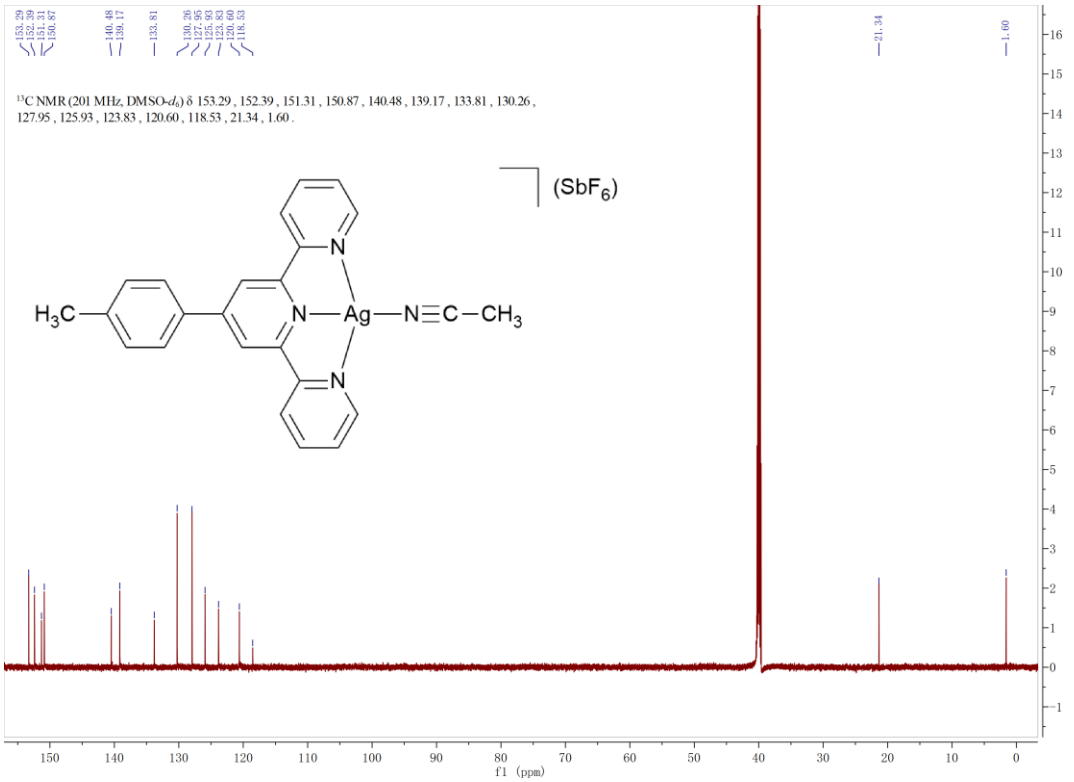

Figure S4 [13]C NMR spectrum of compound **2** in DMSO (201 MHz).

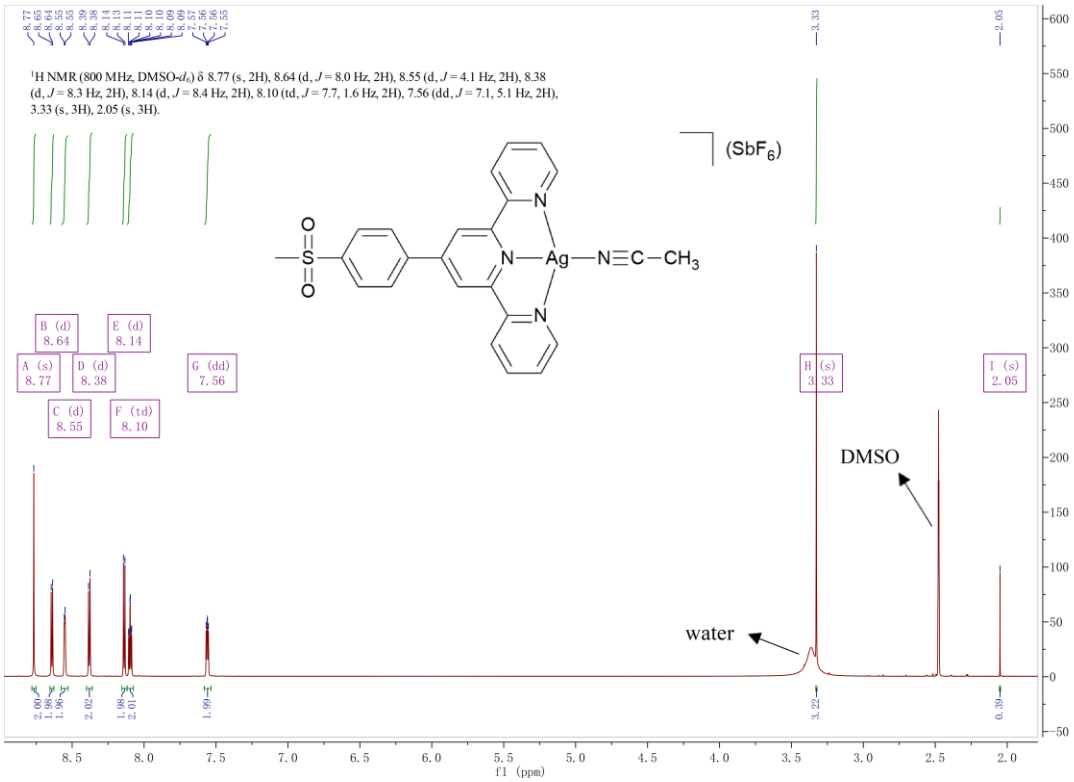

Figure S5 ^{1}H NMR spectrum of compound **3** in DMSO (800 MHz).

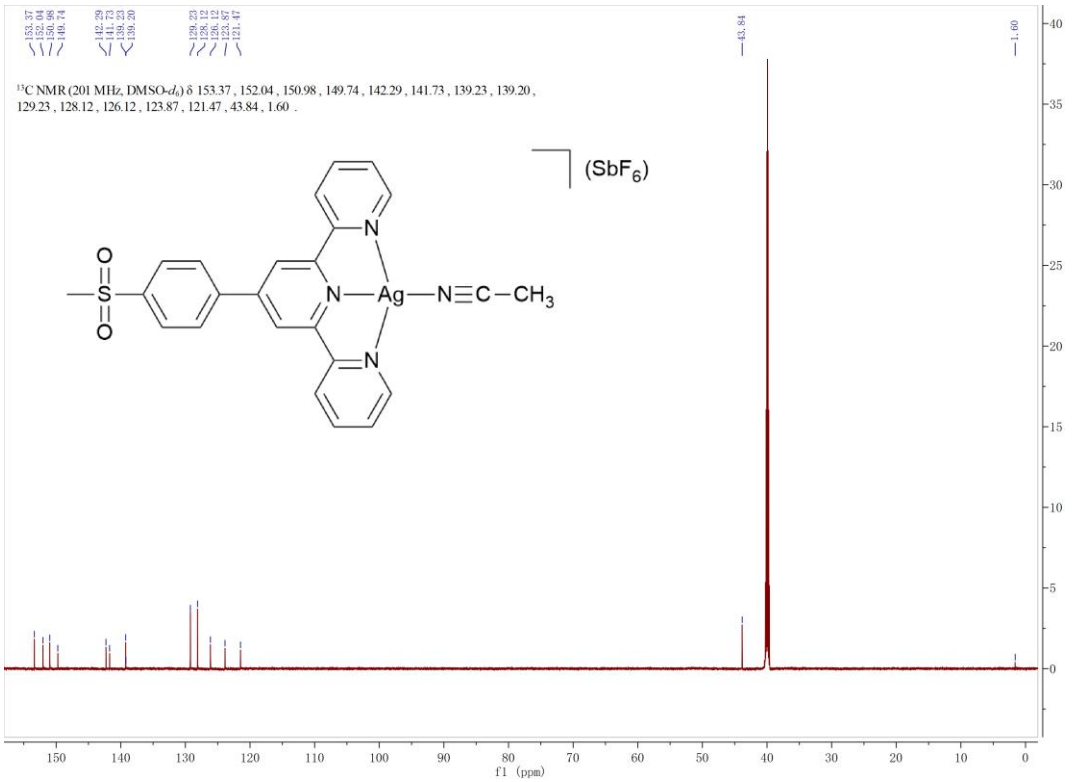

Figure S6 ^{13}C NMR spectrum of compound **3** in DMSO (201 MHz).

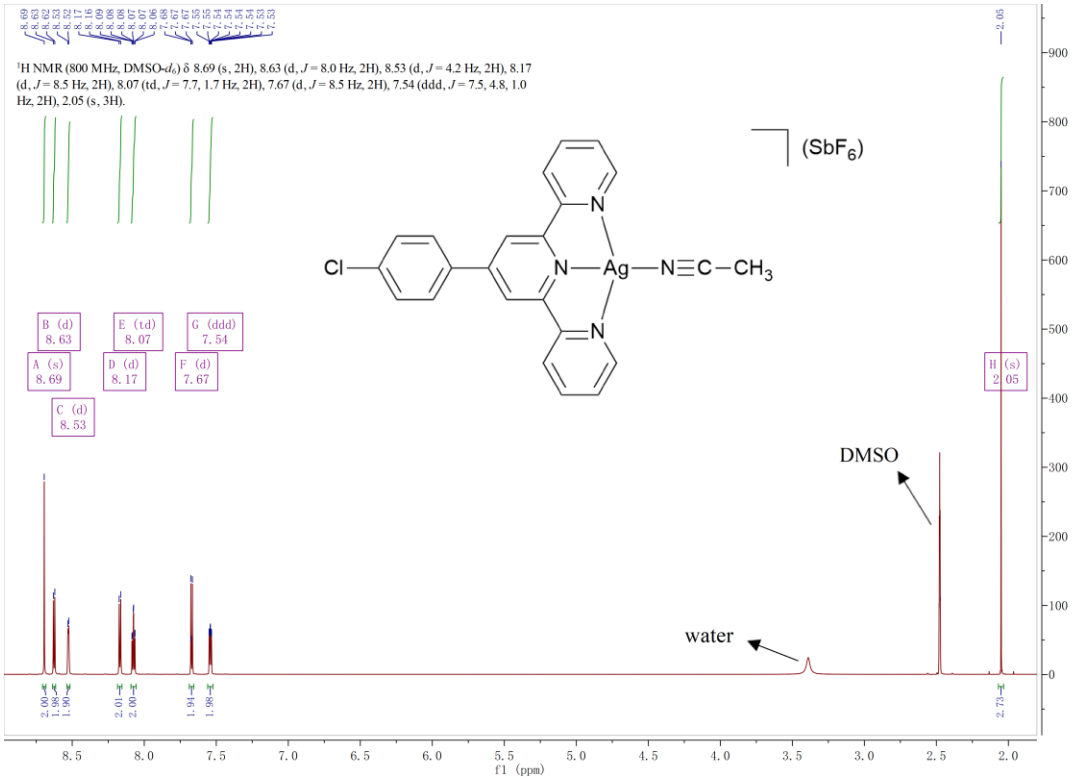

Figure S7 [1]H NMR spectrum of compound **4** in DMSO (800 MHz).

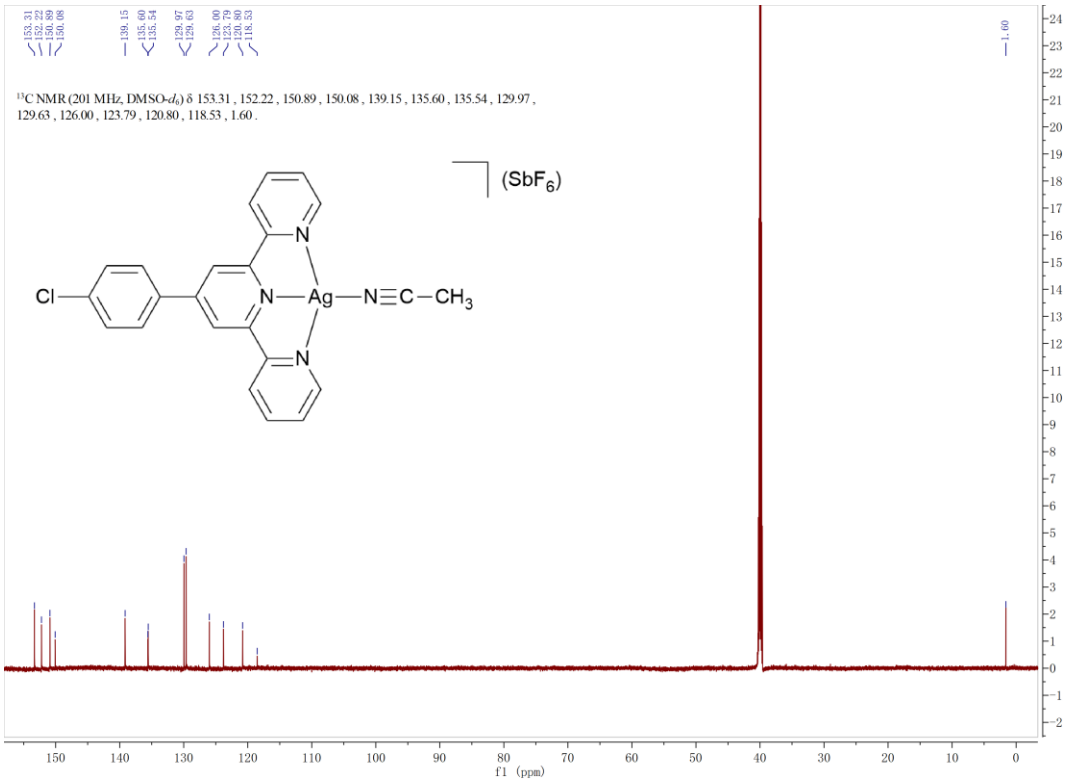

Figure S8 [13]C NMR spectrum of compound **4** in DMSO (201 MHz).

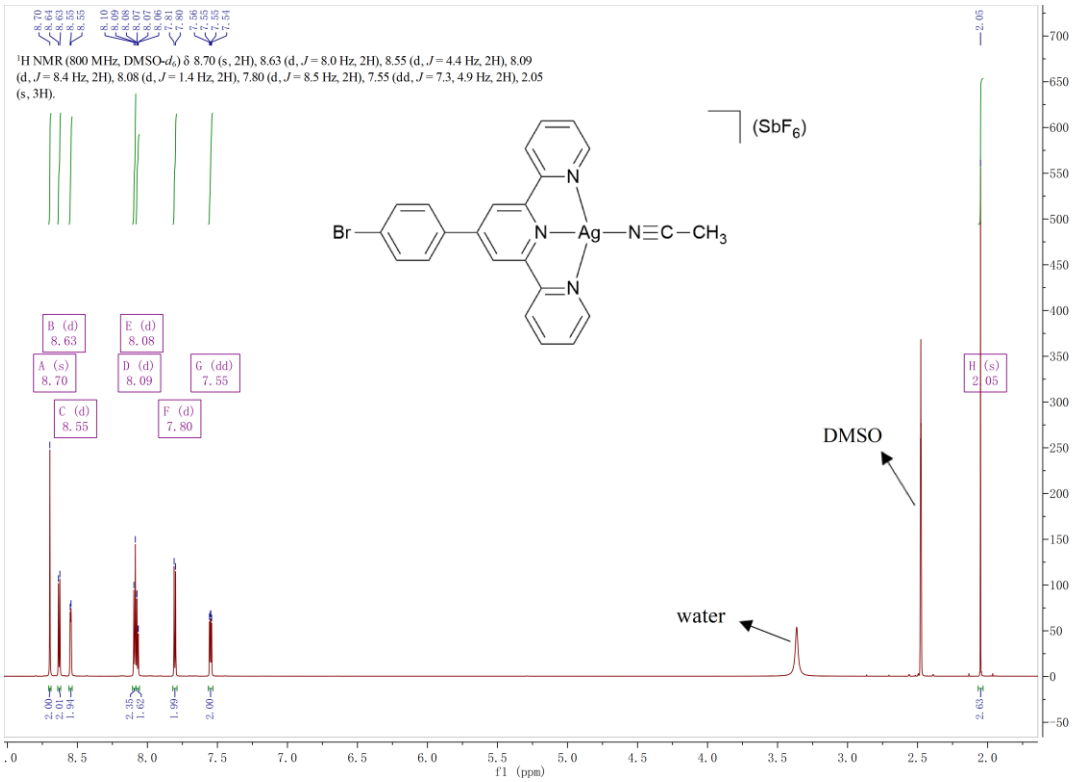

Figure S9 ^{1}H NMR spectrum of compound **5** in DMSO (800 MHz).

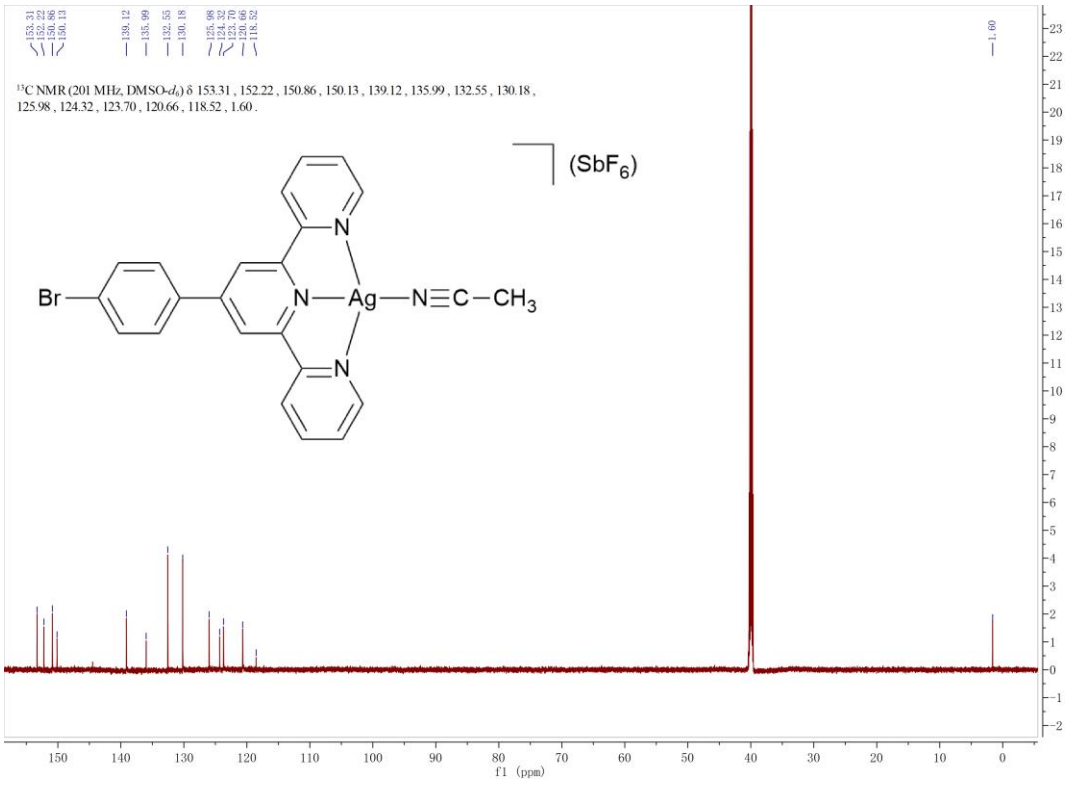

Figure S10 ^{13}C NMR spectrum of compound **5** in DMSO (201 MHz).

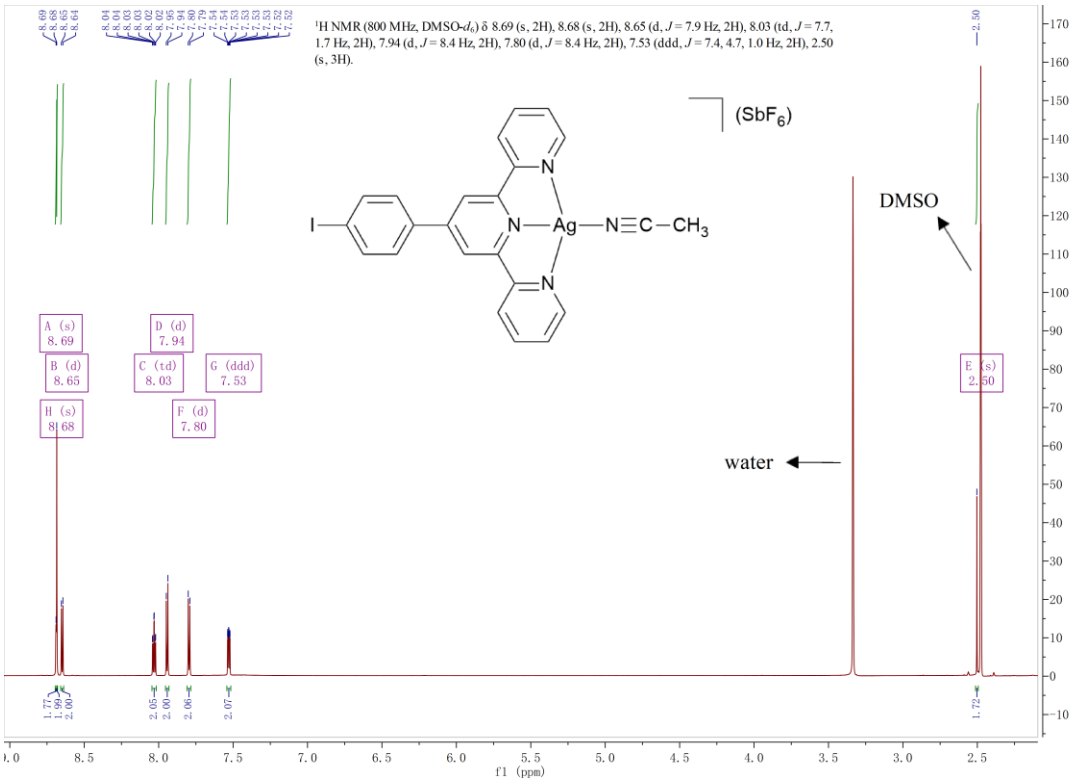

Figure S11 [1]H NMR spectrum of compound **6** in DMSO (800 MHz).

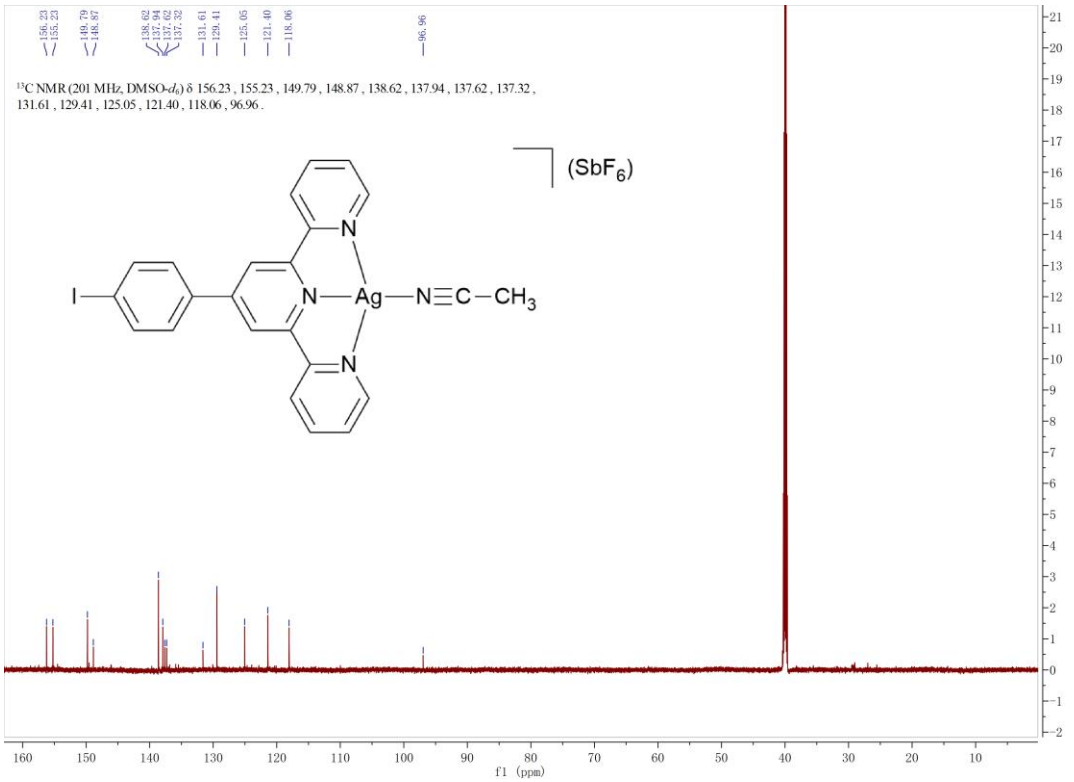

Figure S12 [13]C NMR spectrum of compound **6** in DMSO (201 MHz).

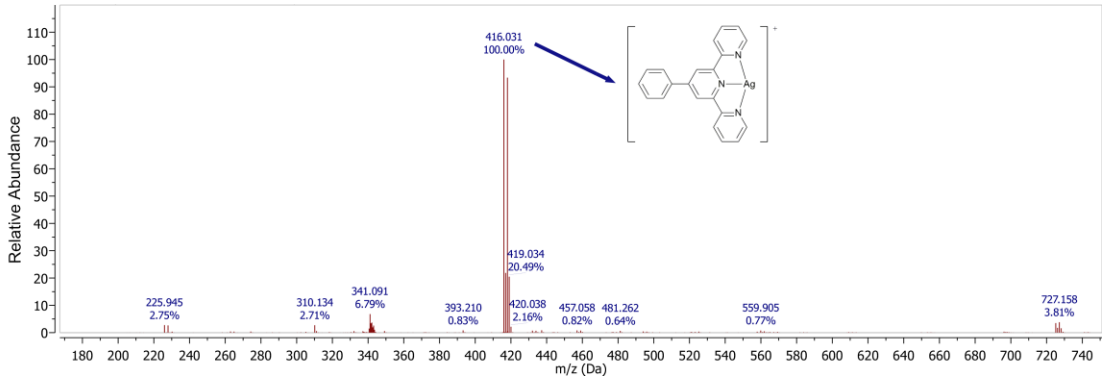

Figure S13 The ESI–MS spectrum of compound **1**.

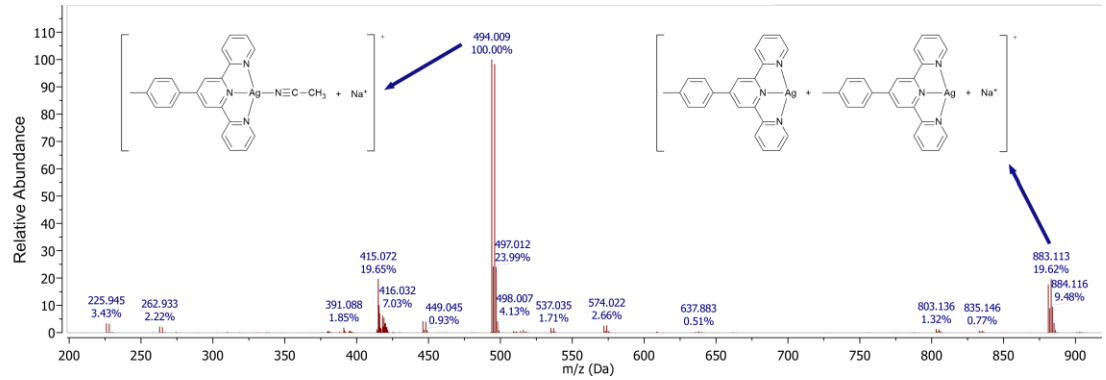

Figure S14 The ESI–MS spectrum of compound **2**.

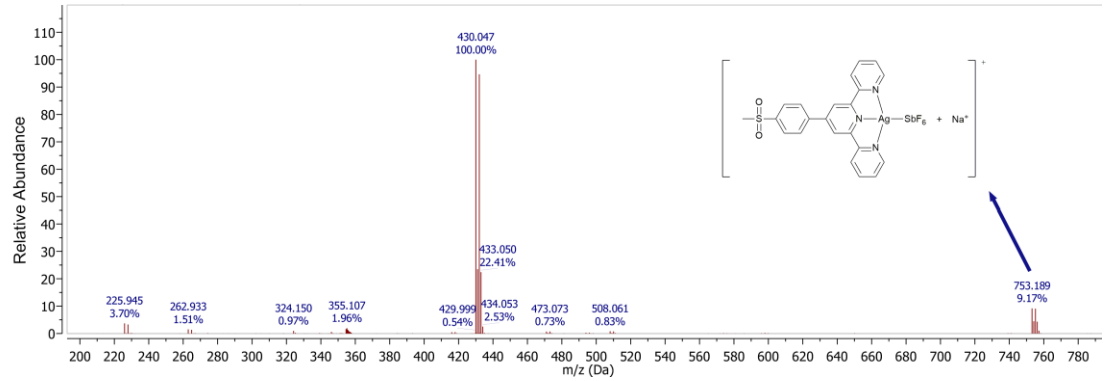

Figure S15 The ESI–MS spectrum of compound **3**.

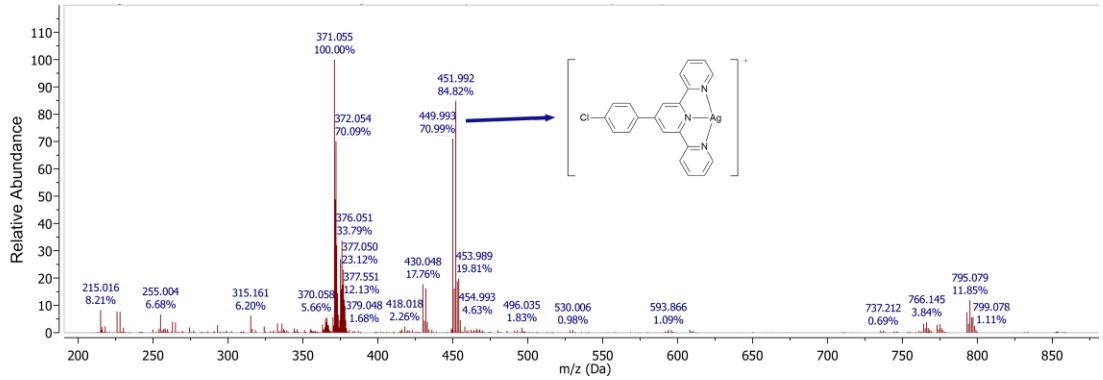

Figure S16 The ESI–MS spectrum of compound **4**.

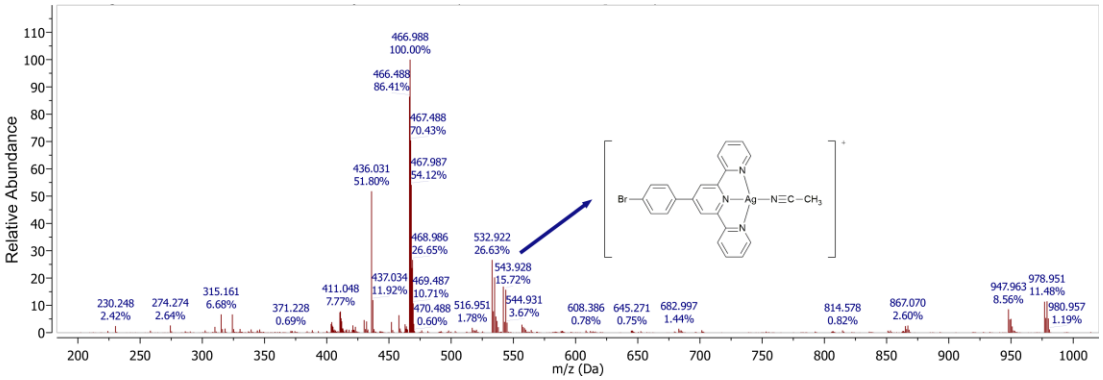

Figure S17 The ESI–MS spectrum of compound **5**.

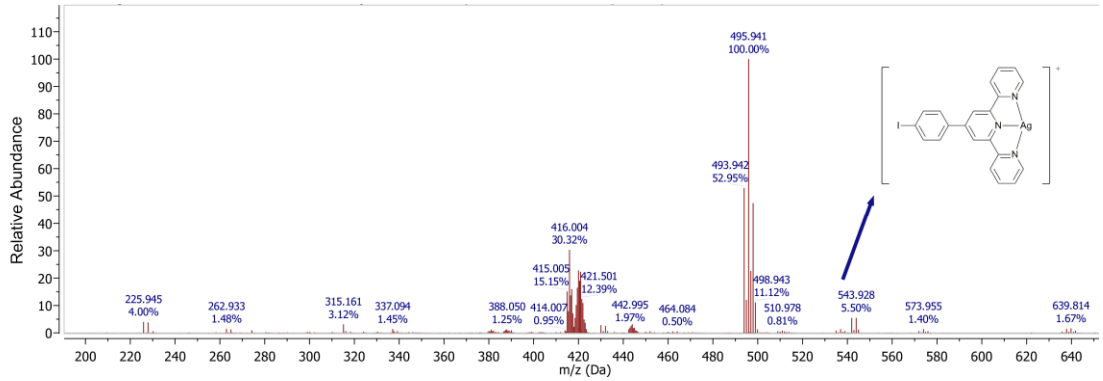

Figure S18 The ESI–MS spectrum of compound **6**.

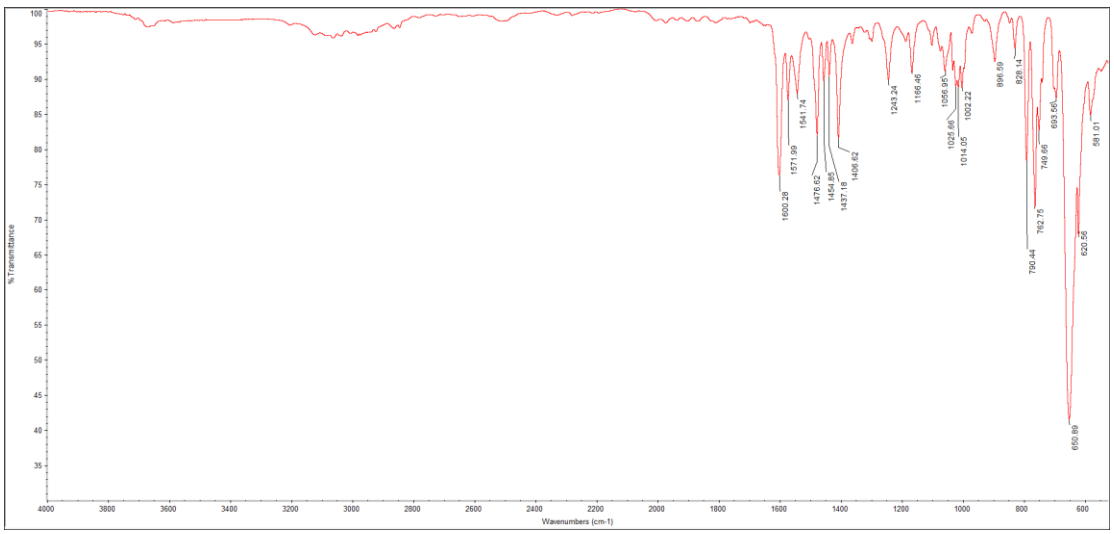

Figure S19 The IR spectrum of compound **1**.

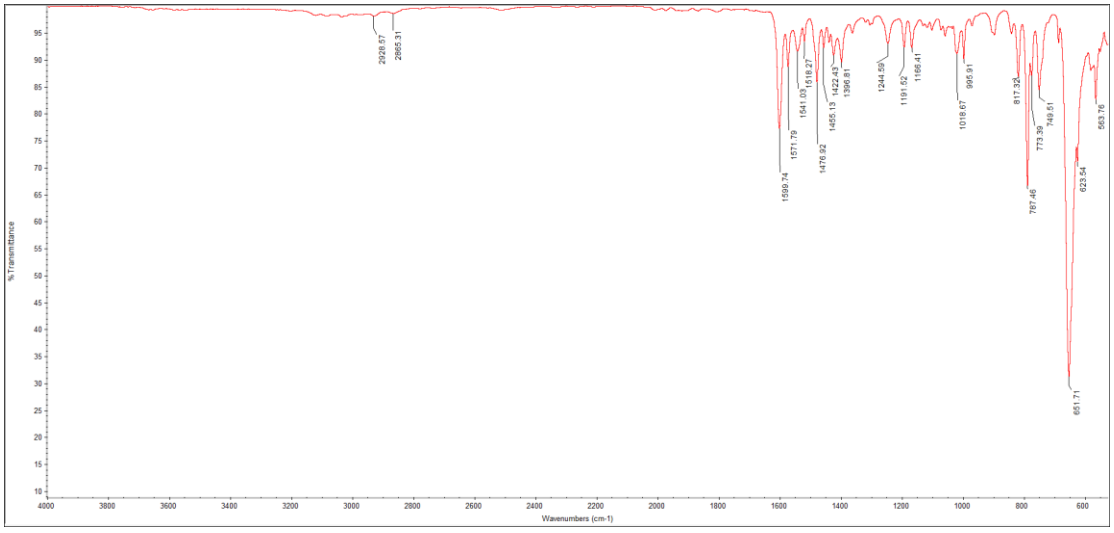

Figure S20 The IR spectrum of compound **2**.

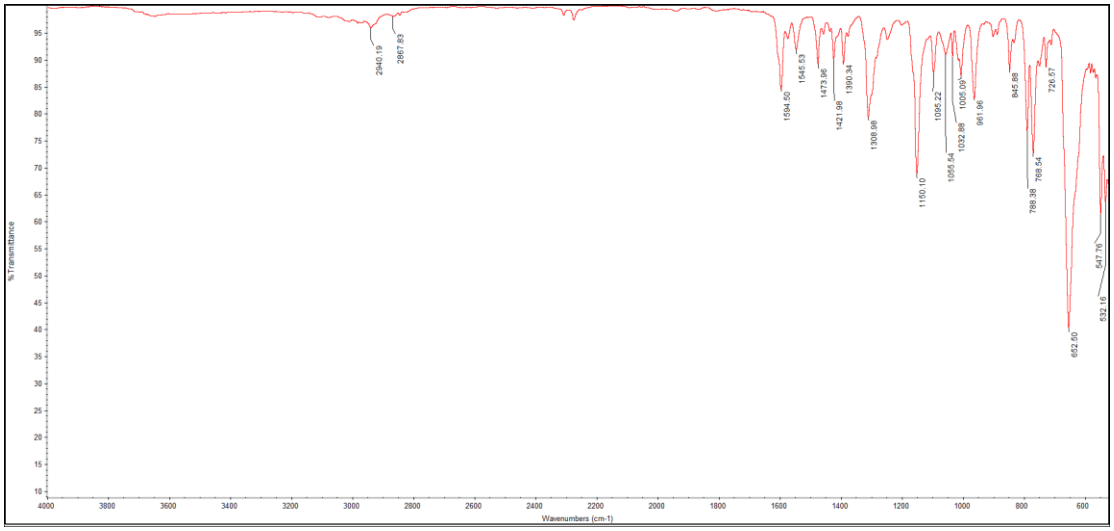

Figure S21 The IR spectrum of compound **3**.

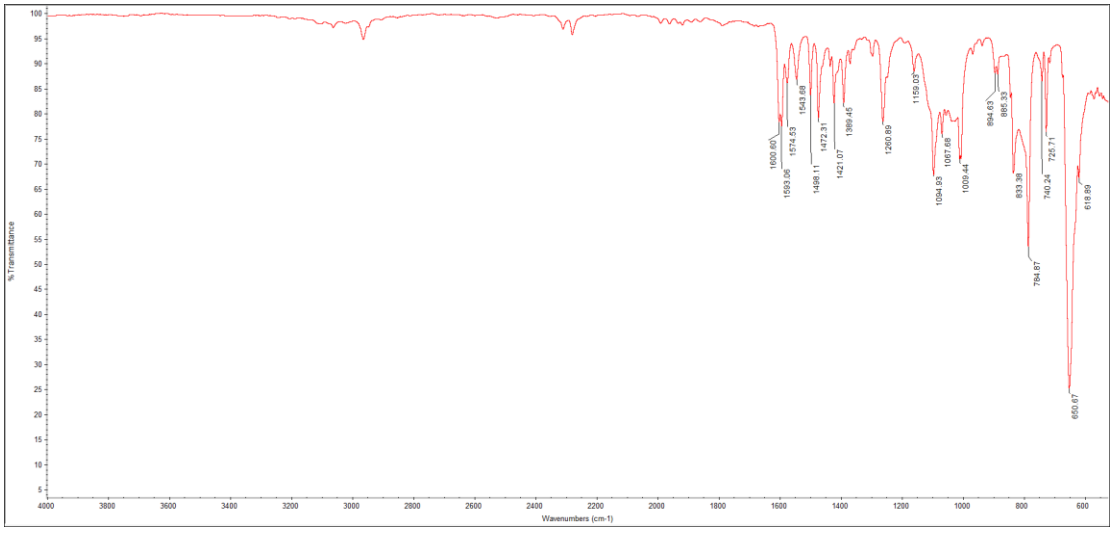

Figure S22 The IR spectrum of compound **4**.

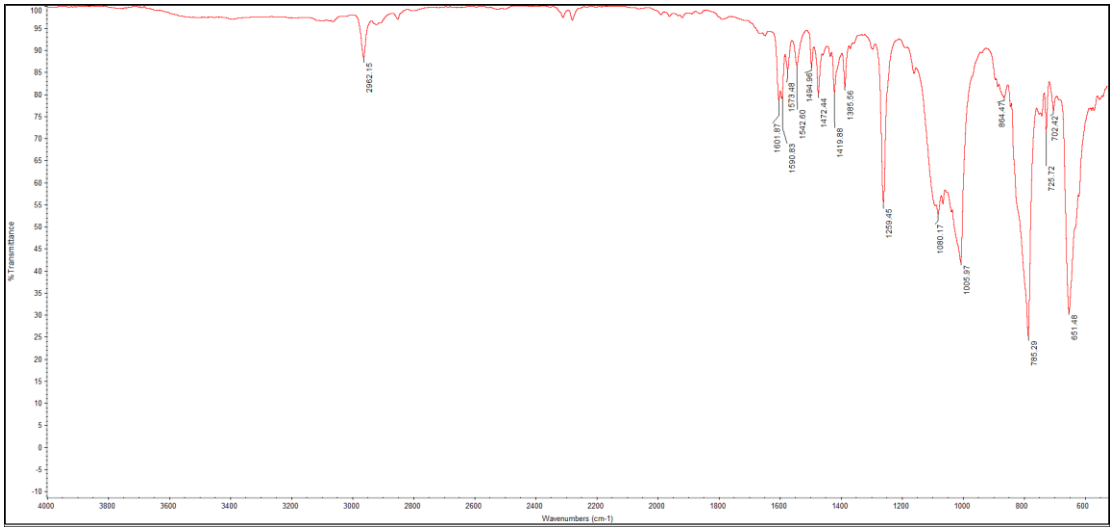

Figure S23 The IR spectrum of compound **5**.

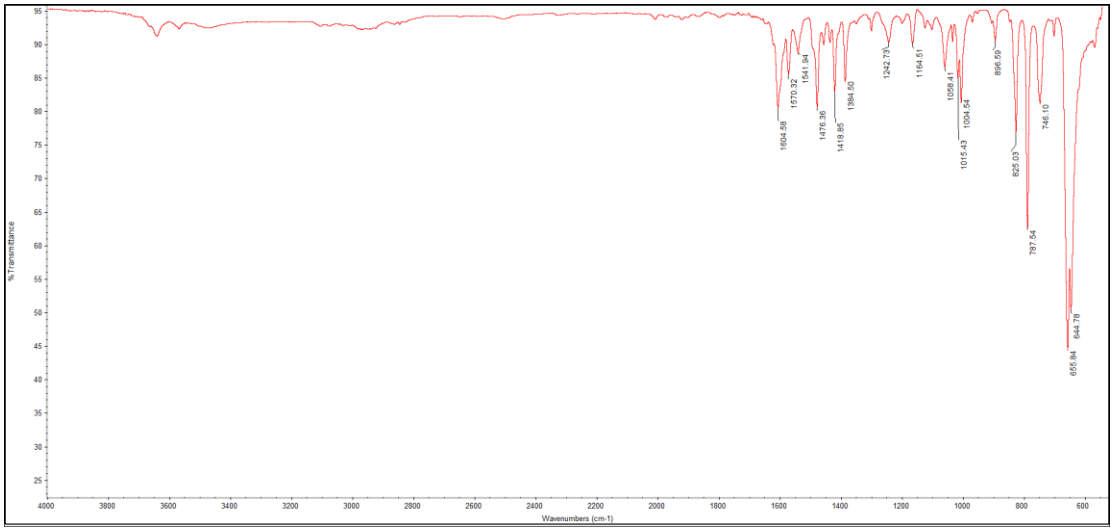

Figure S24 The IR spectrum of compound **6**.

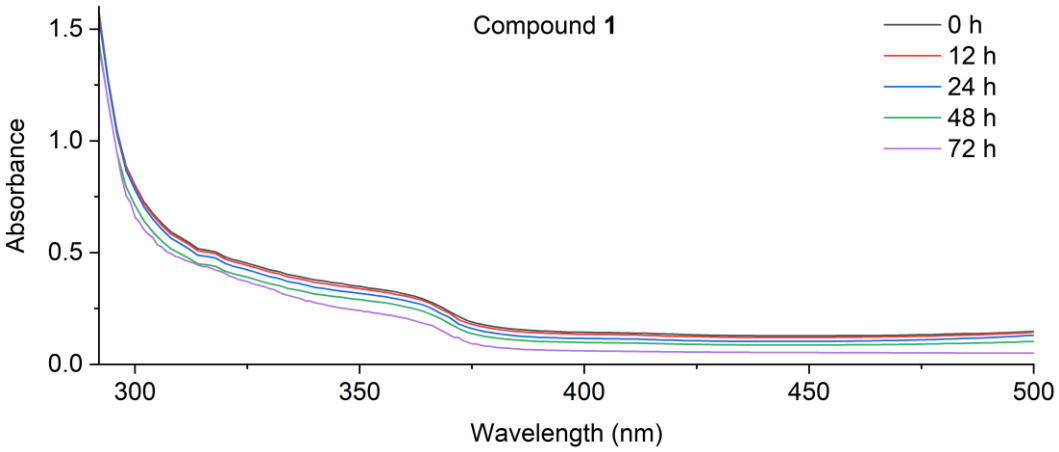

Figure S25 UV−vis spectra of compound **1** in Dulbecco's modified Eagle's medium (DMEM) with 10% of fetal bovine serum (FBS) at 25 °C for a period of 72 h.

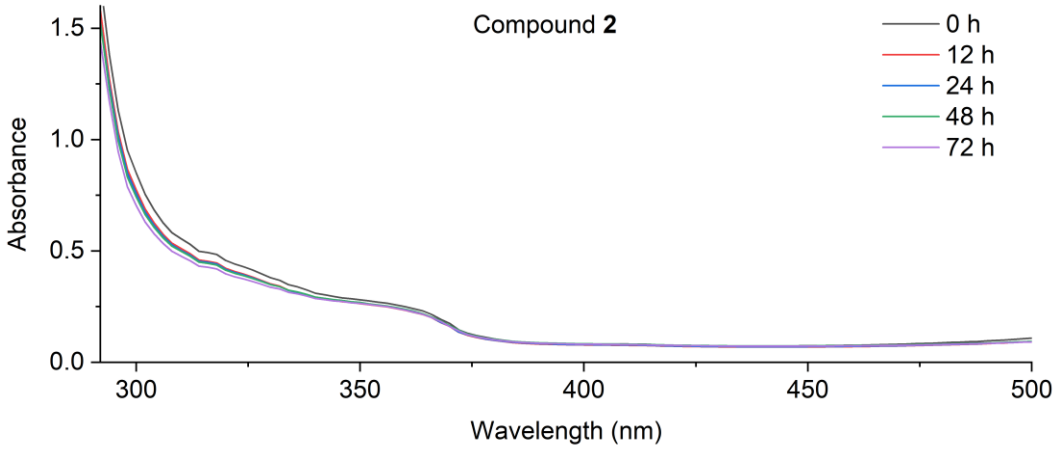

Figure S26 UV−vis spectra of compound **2** in DMEM with 10% FBS at 25 °C for a period of 72 h.

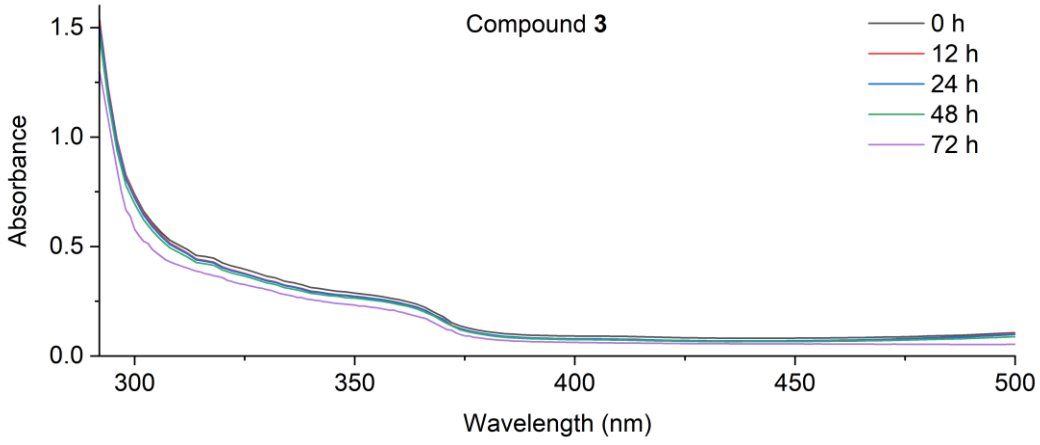

Figure S27 UV−vis spectra of compound **3** in DMEM with 10% FBS at 25 °C for a period of 72 h.

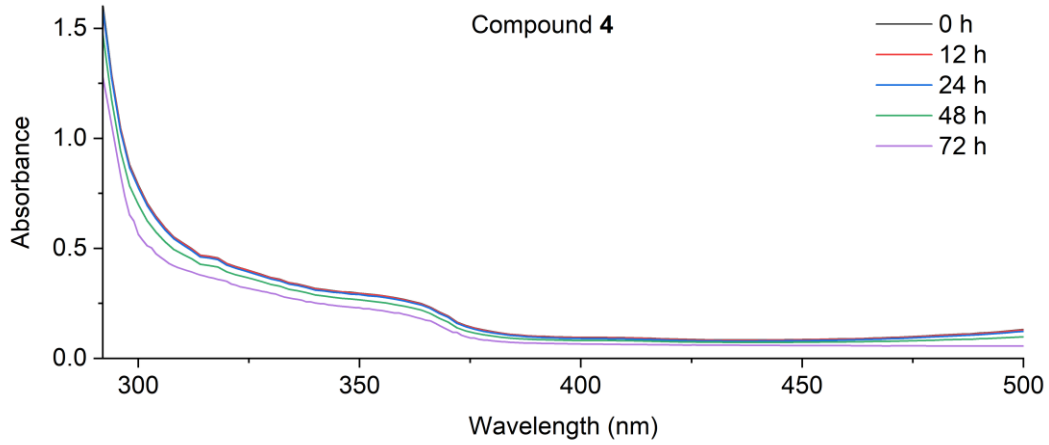

Figure S28 UV−vis spectra of compound **4** in DMEM with 10% FBS at 25 °C for a period of 72 h.

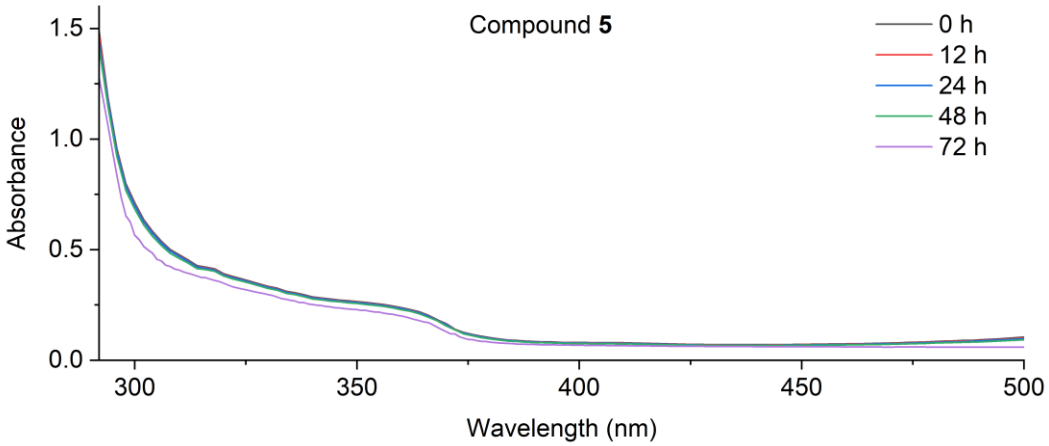

Figure S29 UV−vis spectra of compound **5** in DMEM with 10% FBS at 25 °C for a period of 72 h.

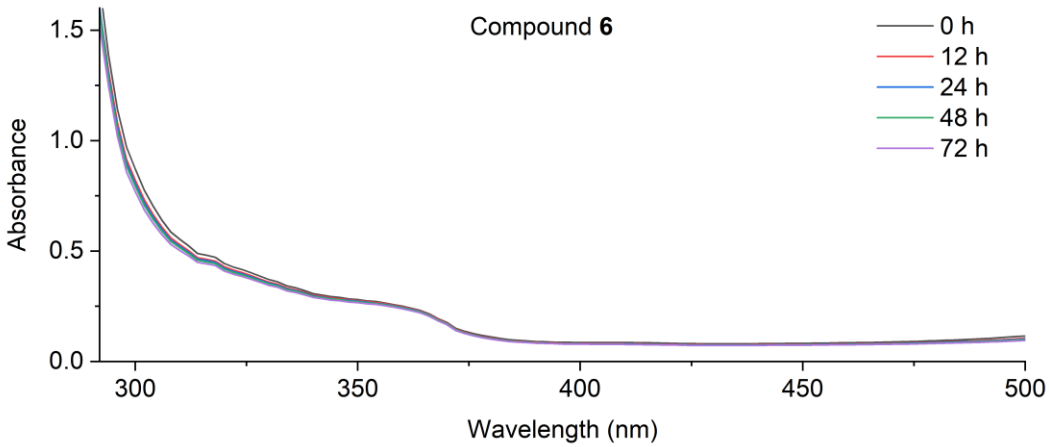

Figure S30 UV−vis spectra of compound **6** in DMEM with 10% FBS at 25 °C for a period of 72 h.

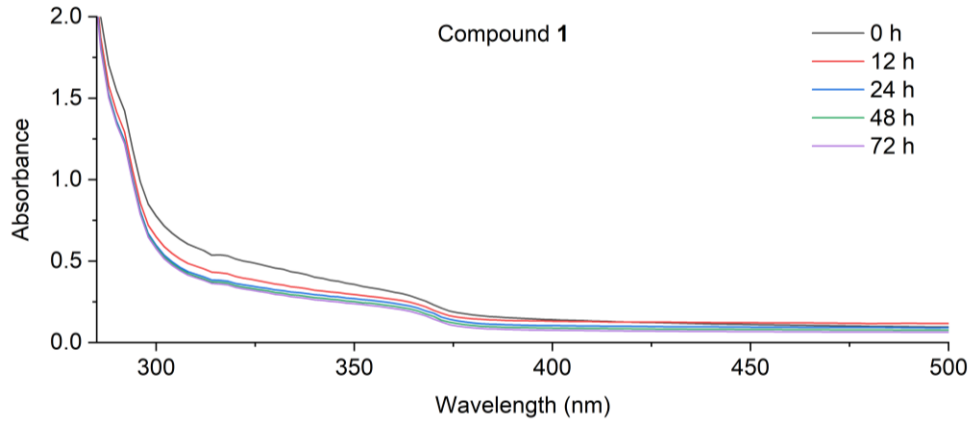

Figure S31 UV−vis spectra of compound **1** in bovine serum albumin (BSA) in Tris-HCl buffer at 25 °C for a period of 72 h.

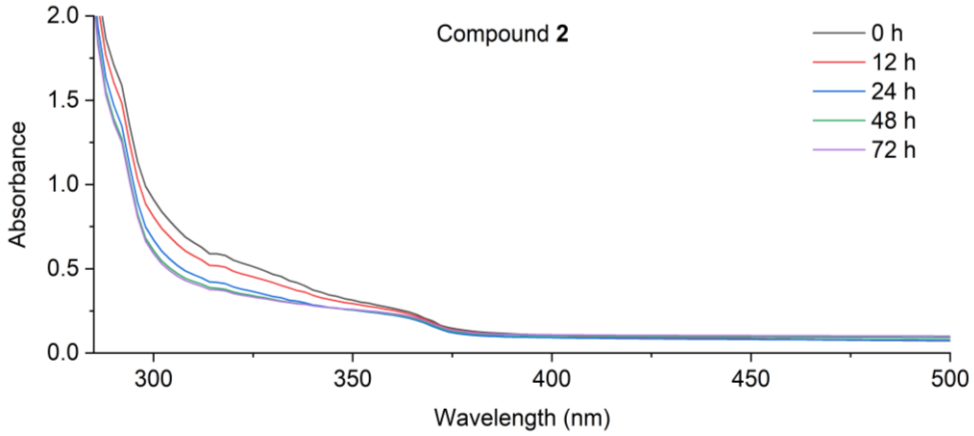

Figure S32 UV−vis spectra of compound **2** in bovine serum albumin (BSA) in Tris-HCl buffer at 25 °C for a period of 72 h.

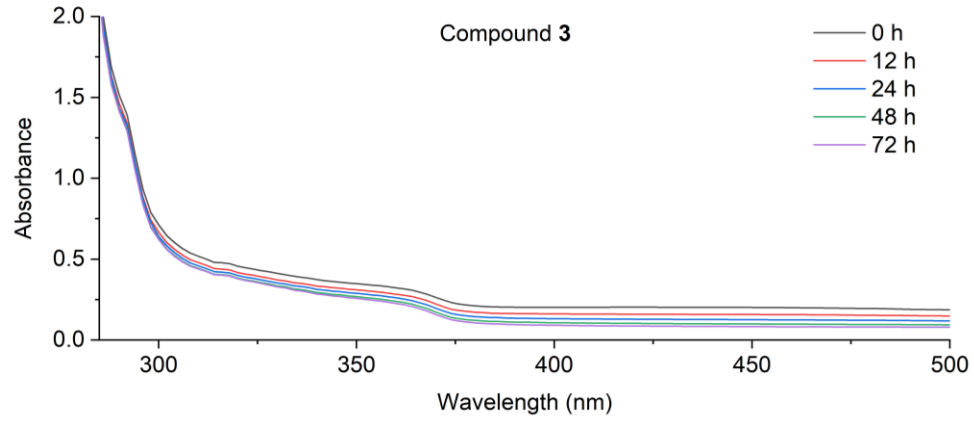

Figure S33 UV−vis spectra of compound **3** in bovine serum albumin (BSA) in Tris-HCl buffer at 25 °C for a period of 72 h.

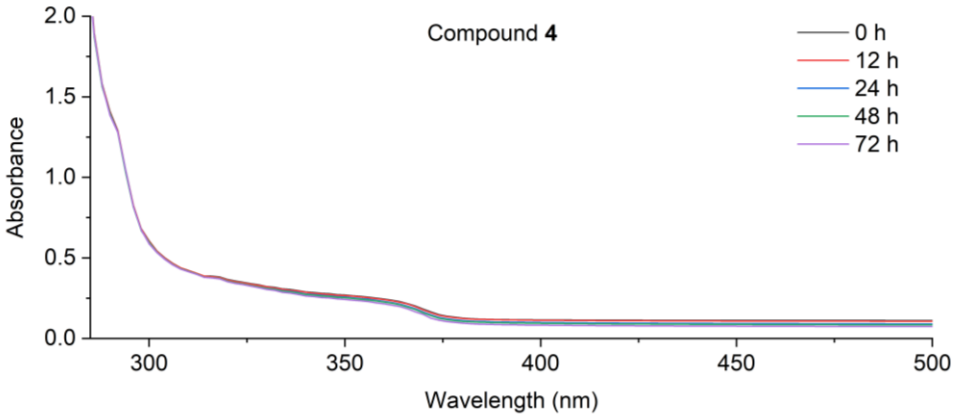

Figure S34 UV−vis spectra of compound **4** in bovine serum albumin (BSA) in Tris-HCl buffer at 25 °C for a period of 72 h.

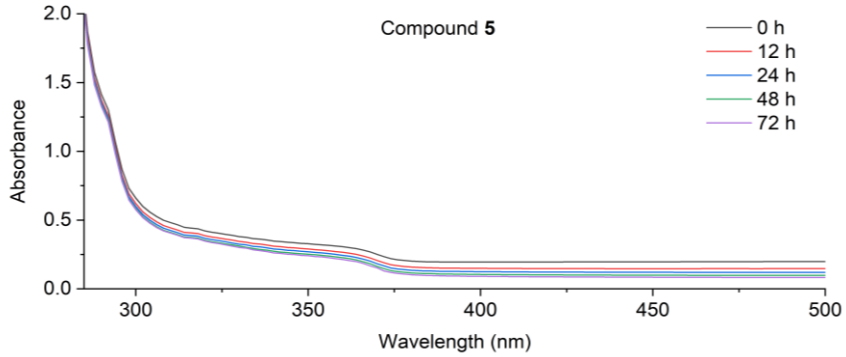

Figure S35 UV−vis spectra of compound **5** in bovine serum albumin (BSA) in Tris-HCl buffer at 25 °C for a period of 72 h.

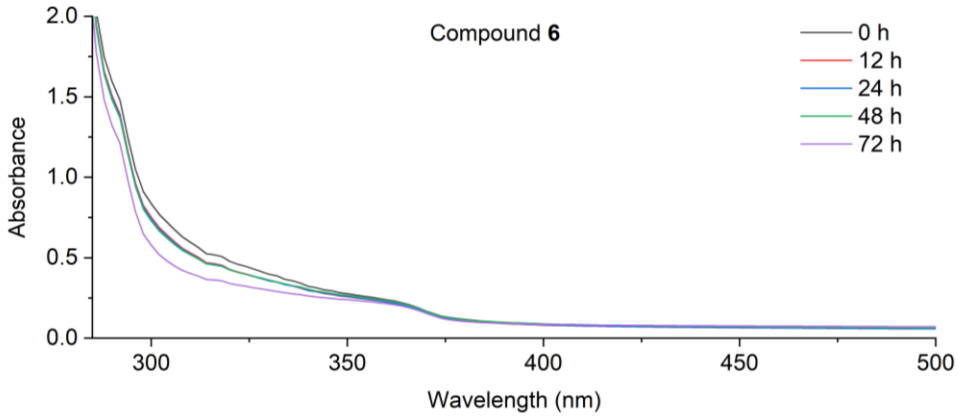

Figure S36 UV−vis spectra of compound **6** in bovine serum albumin (BSA) in Tris-HCl buffer at 25 °C for a period of 72 h.

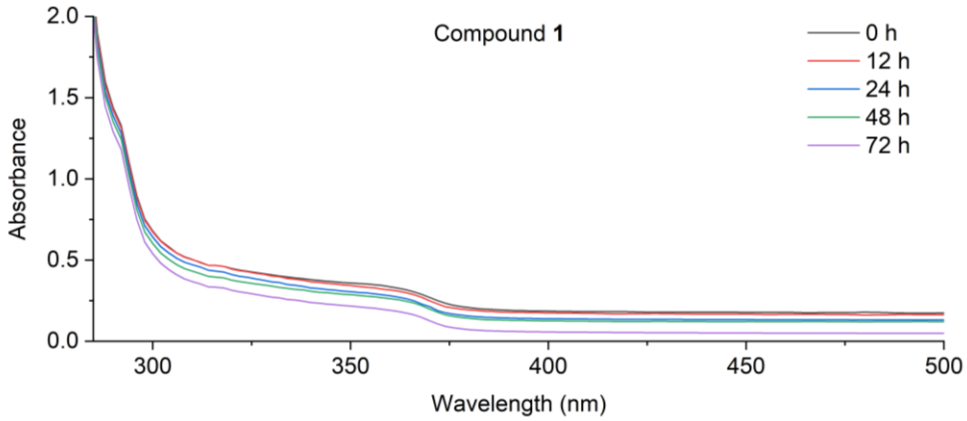

Figure S37 UV−vis spectra of compound **1** in glutathione (GSH) in Tris-HCl buffer at 25 °C for a period of 72 h.

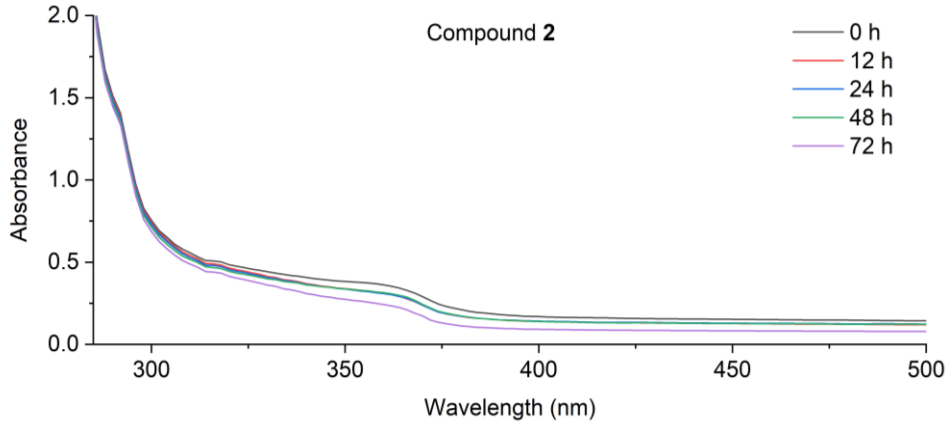

Figure S38 UV−vis spectra of compound **2** in glutathione (GSH) in Tris-HCl buffer at 25 °C for a period of 72 h.

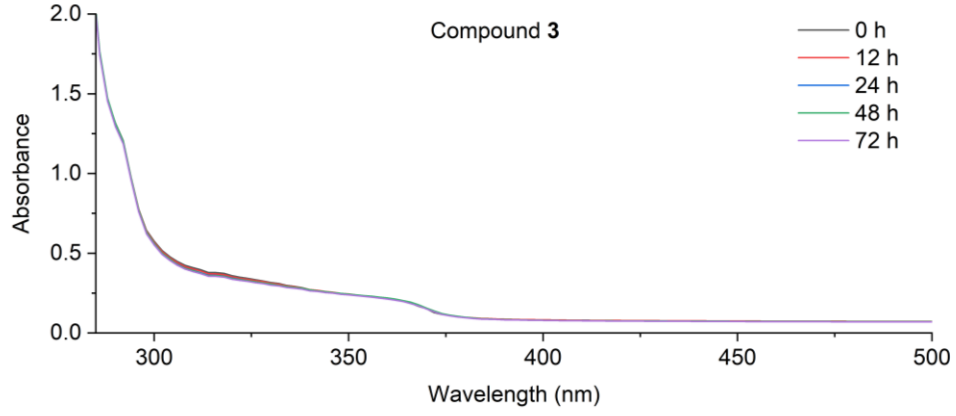

Figure S39 UV−vis spectra of compound **3** in glutathione (GSH) in Tris-HCl buffer at 25 °C for a period of 72 h.

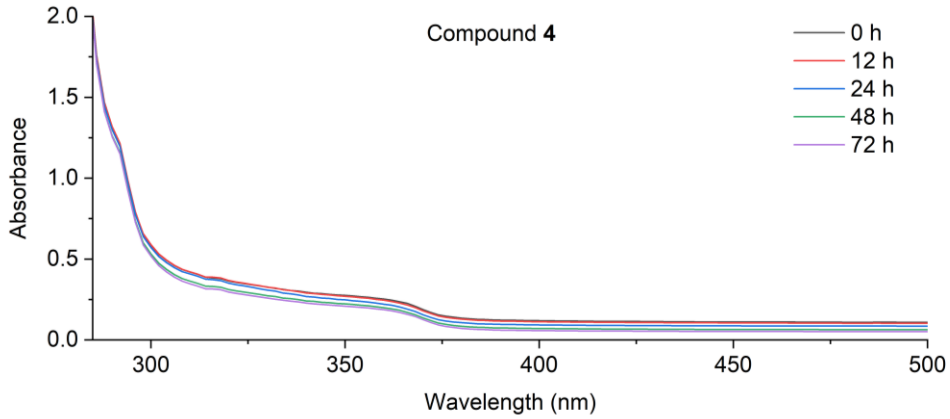

Figure S40 UV−vis spectra of compound **4** in glutathione (GSH) in Tris-HCl buffer at 25 °C for a period of 72 h.

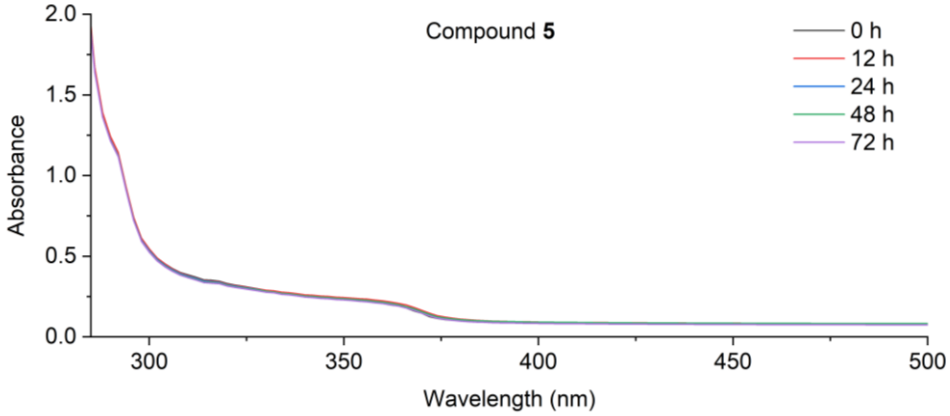

Figure S41 UV−vis spectra of compound **5** in glutathione (GSH) in Tris-HCl buffer at 25 °C for a period of 72 h.

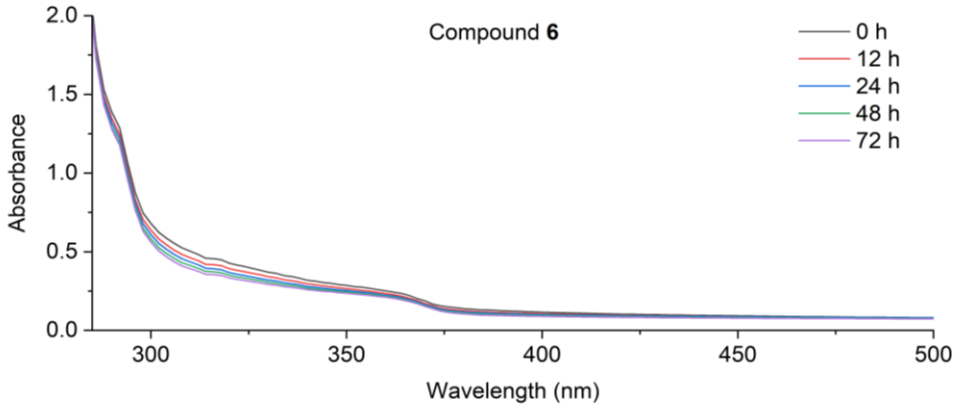

Figure S42 UV−vis spectra of compound **6** in glutathione (GSH) in Tris-HCl buffer at 25 °C for a period of 72 h.

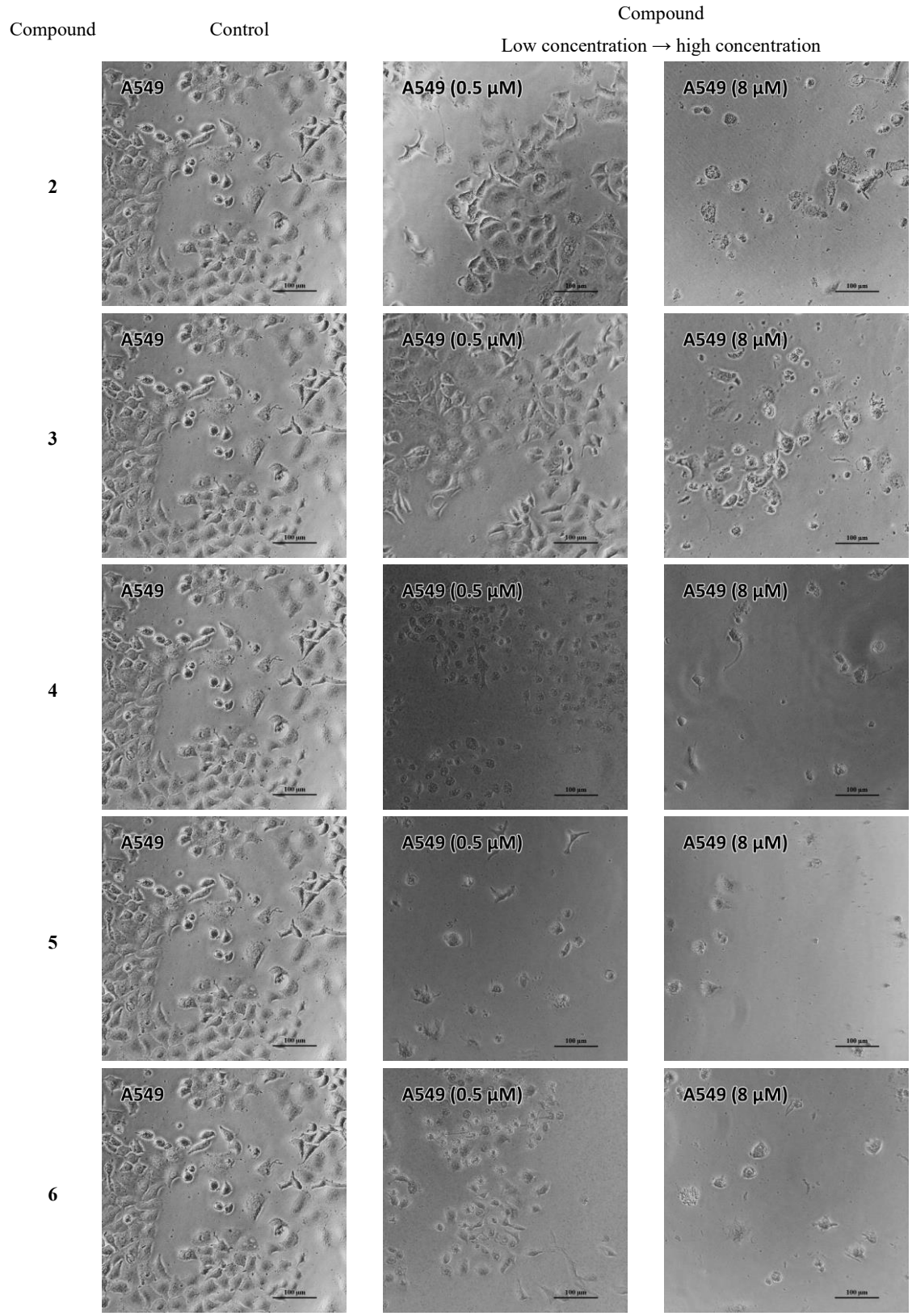

Figure S43 The microscopic images of A549 cells treated with increased concentrations of compounds **2**–**6**.

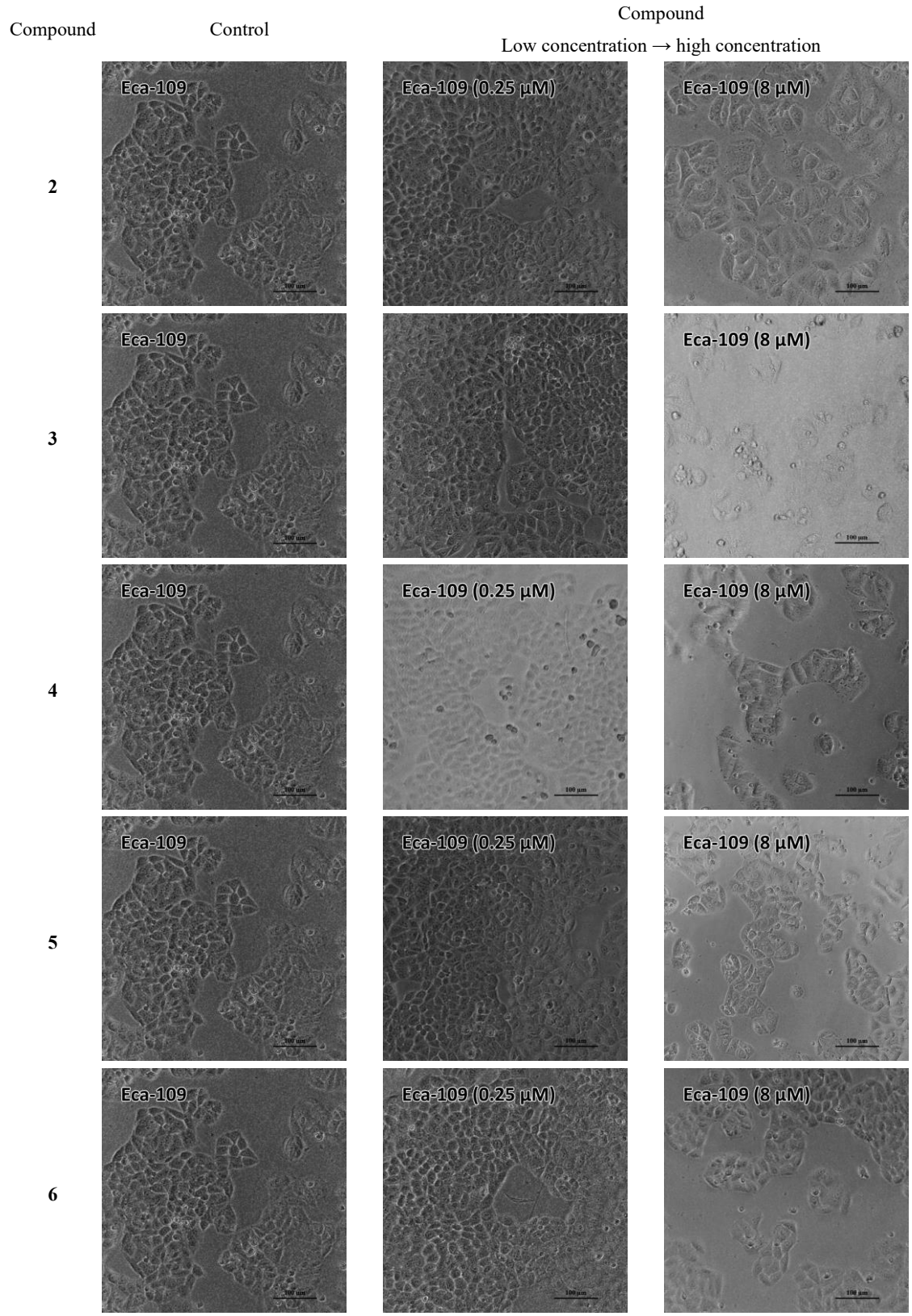

Figure S44 The microscopic images of Eca-109 cells treated with increased concentrations of compounds **2**–**6**.

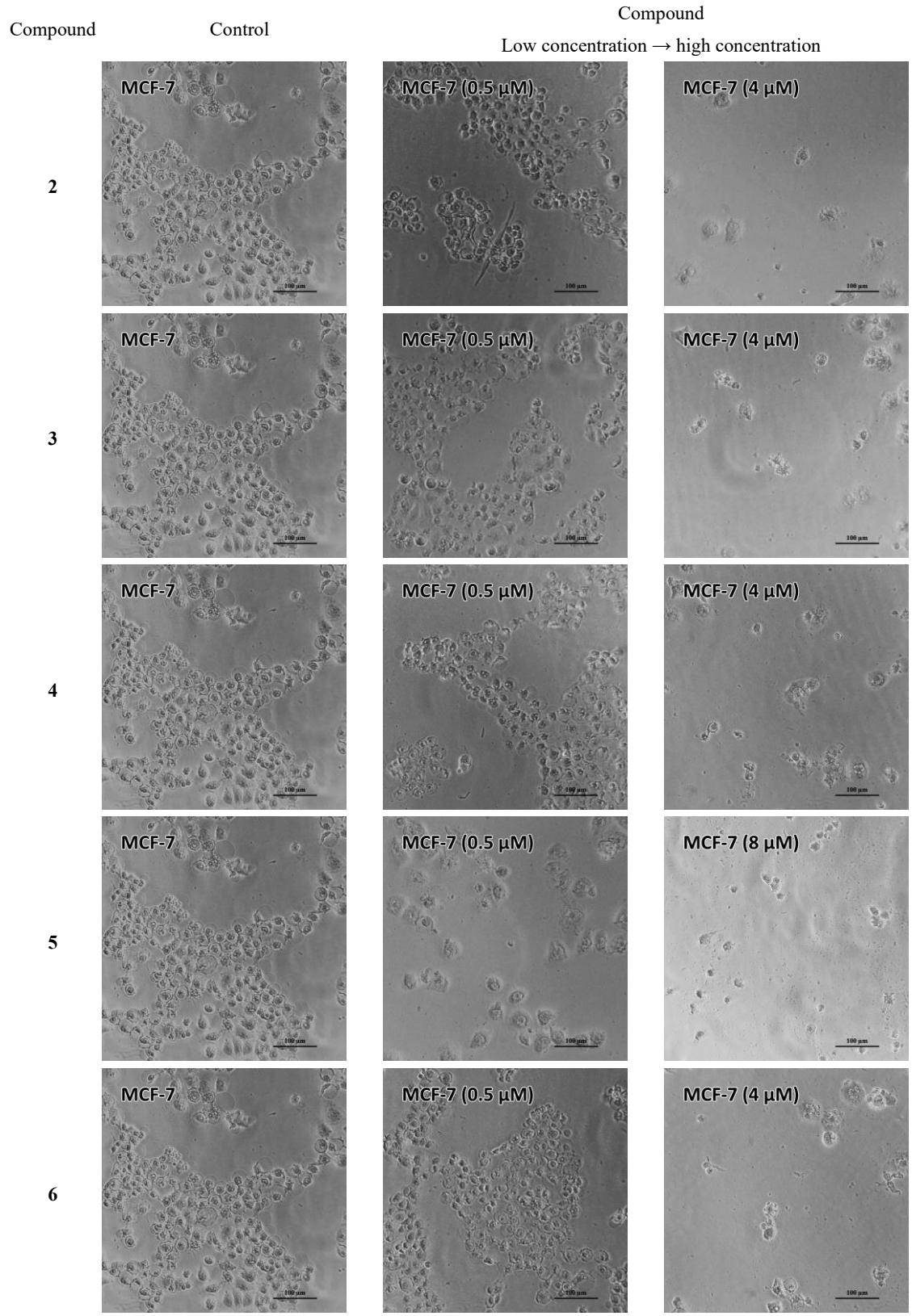

Figure S45 The microscopic images of MCF-7 cells treated with increased concentrations of compounds **2**–**6**.

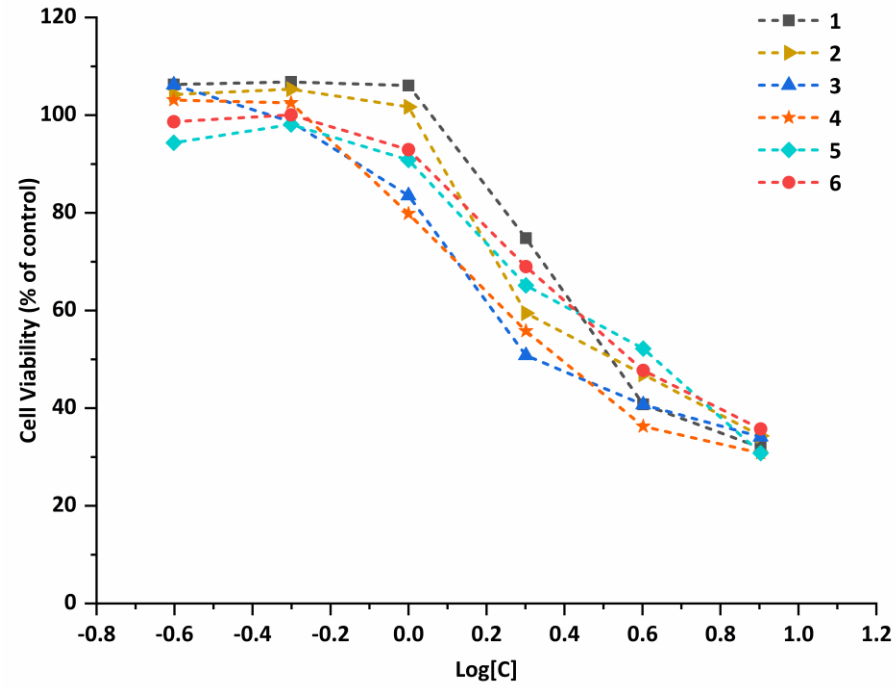

Figure S46 The plots of cell viability *vs.* the concentration of compounds **1**–**6** against Eca-109 cells.

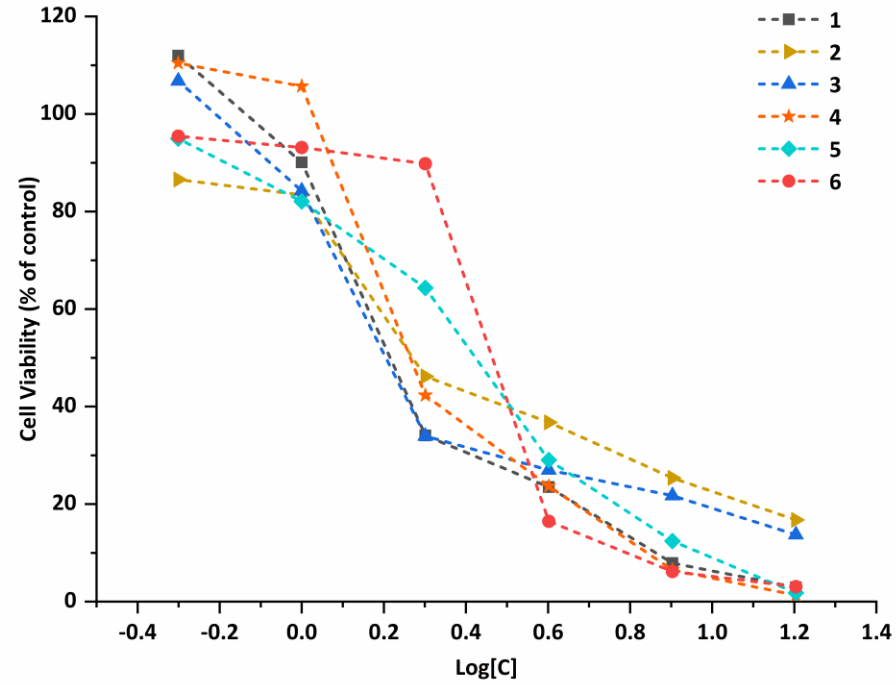

Figure S47 The plots of cell viability *vs.* the concentration of compounds **1**–**6** against MCF-7 cells.

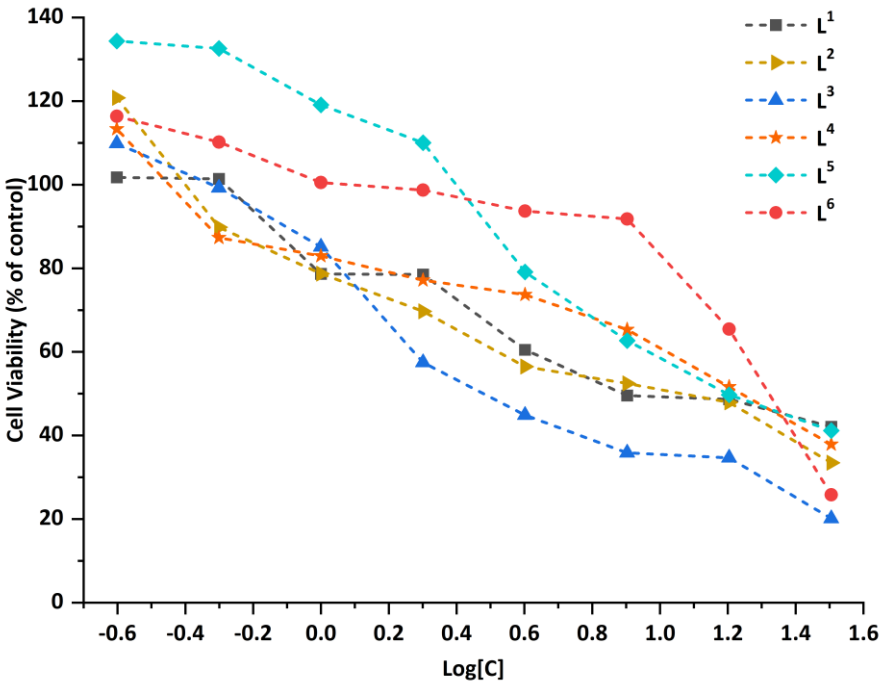

Figure S48 The plots of cell viability *vs.* the concentration of ligands $\mathbf{L^1}$–$\mathbf{L^6}$ against A549 cells.

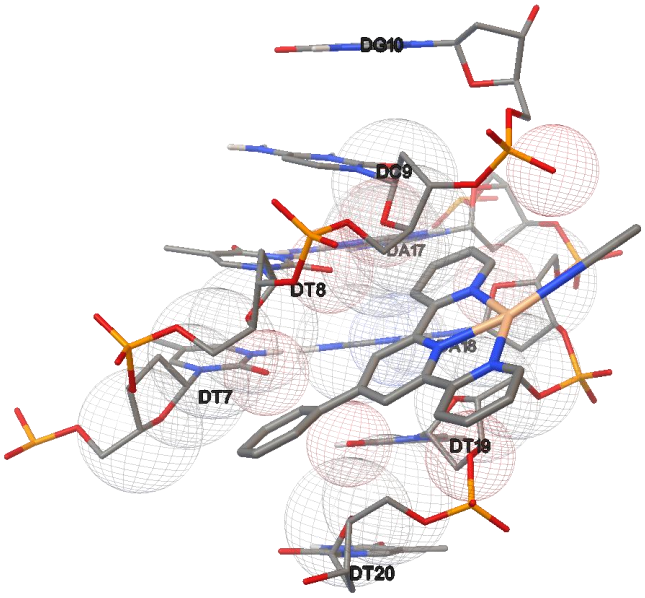

Figure S49 The most favorable orientation of compound **1** with the minor groove of the B-DNA (PDB ID: 1BNA).

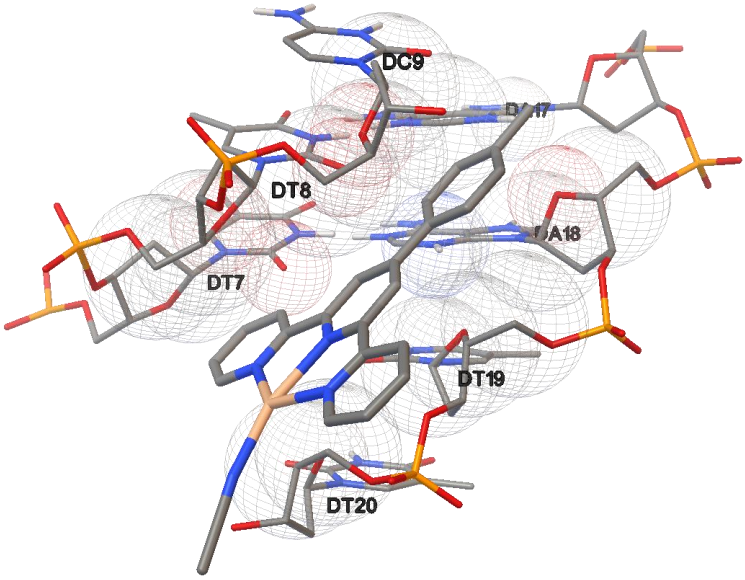

Figure S50 The most favorable orientation of compound **2** with the minor groove of the B-DNA (PDB ID: 1BNA).

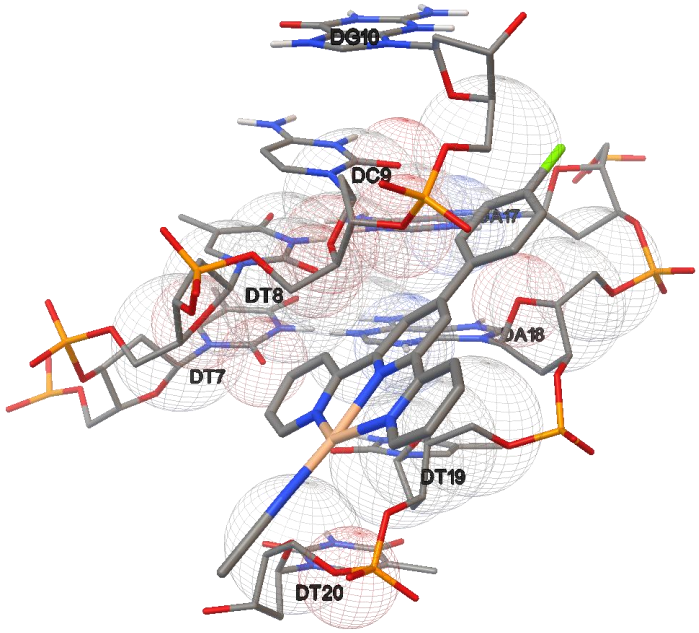

Figure S51 The most favorable orientation of compound **4** with the minor groove of the B-DNA (PDB ID: 1BNA).

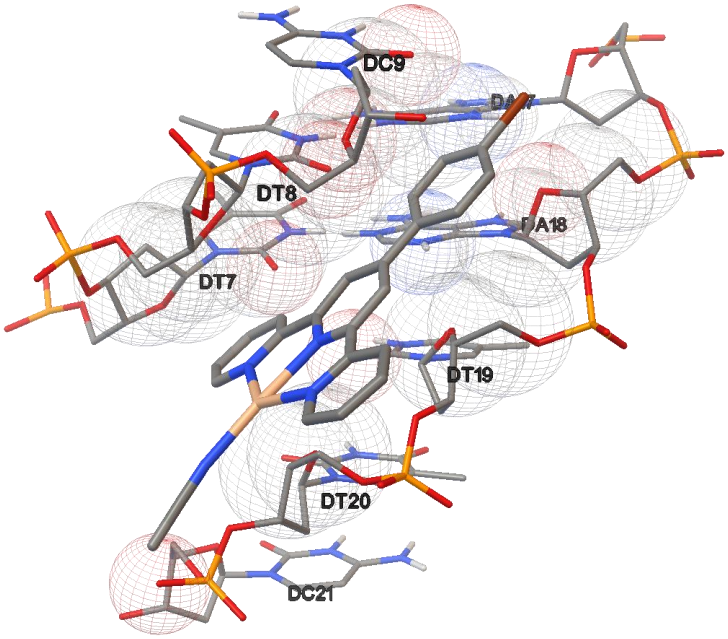

Figure S52 The most favorable orientation of compound **5** with the minor groove of the B-DNA (PDB ID: 1BNA).

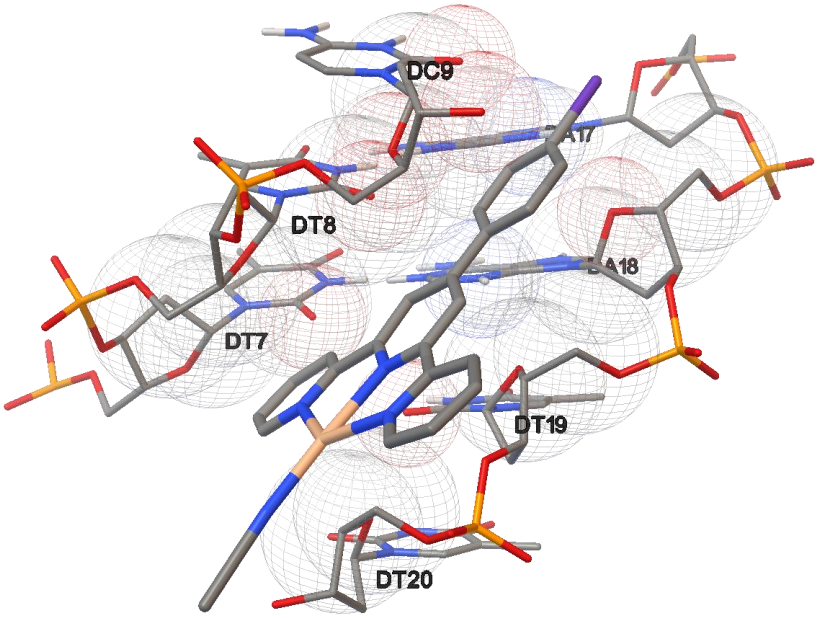

Figure S53 The most favorable orientation of compound **6** with the minor groove of the B-DNA (PDB ID: 1BNA).

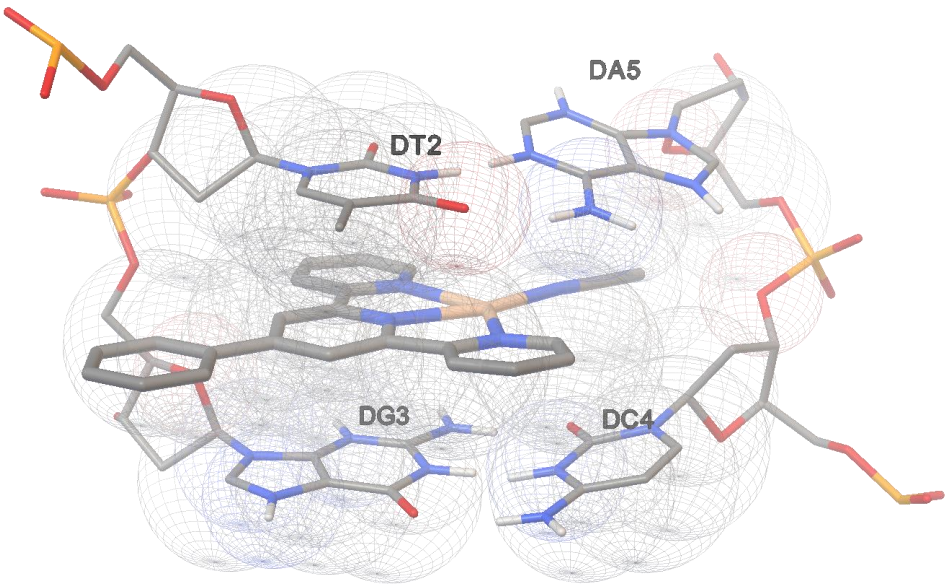

Figure S54 The most favorable orientation of compound **1** intercalating with the DNA (4JD8).

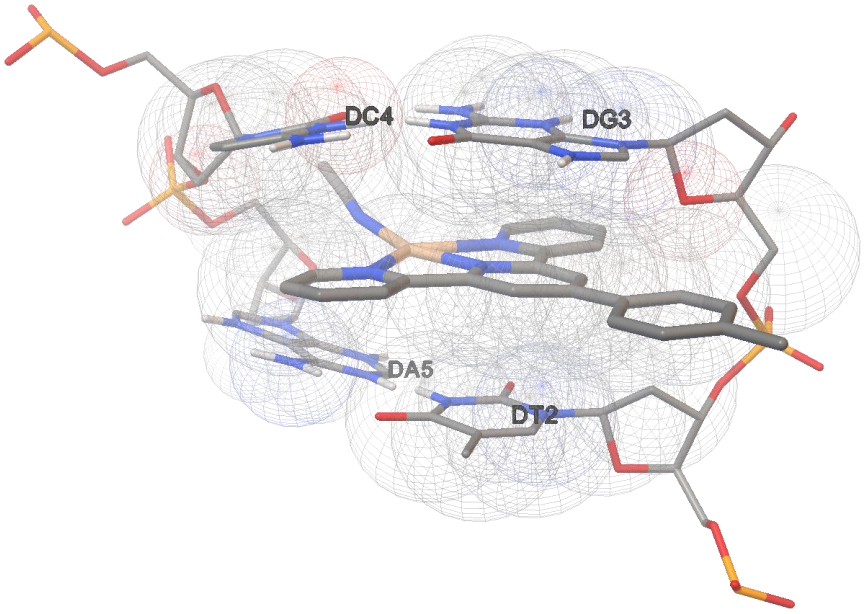

Figure S55 The most favorable orientation of compound **2** intercalating with the DNA (4JD8).

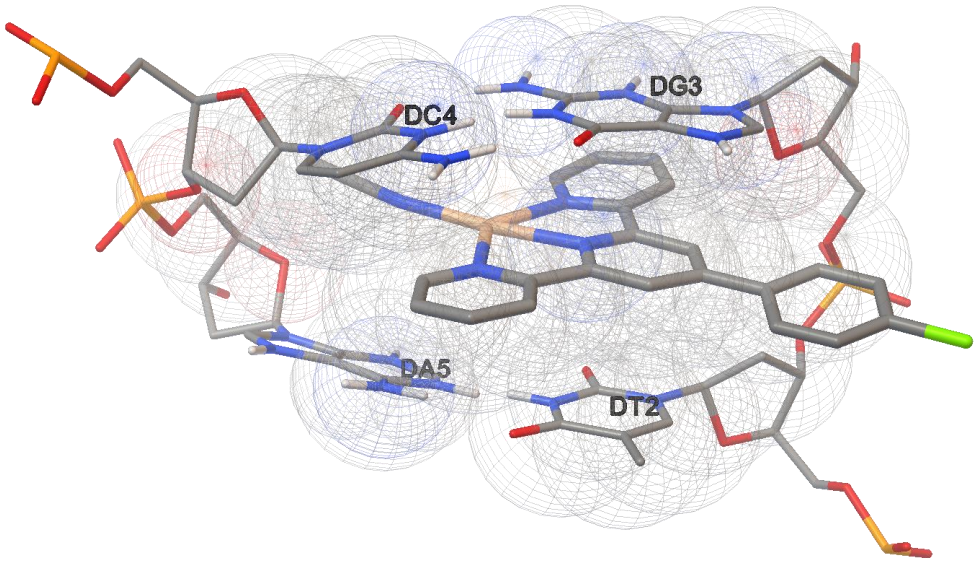

Figure S56 The most favorable orientation of compound **4** intercalating with the DNA (4JD8).

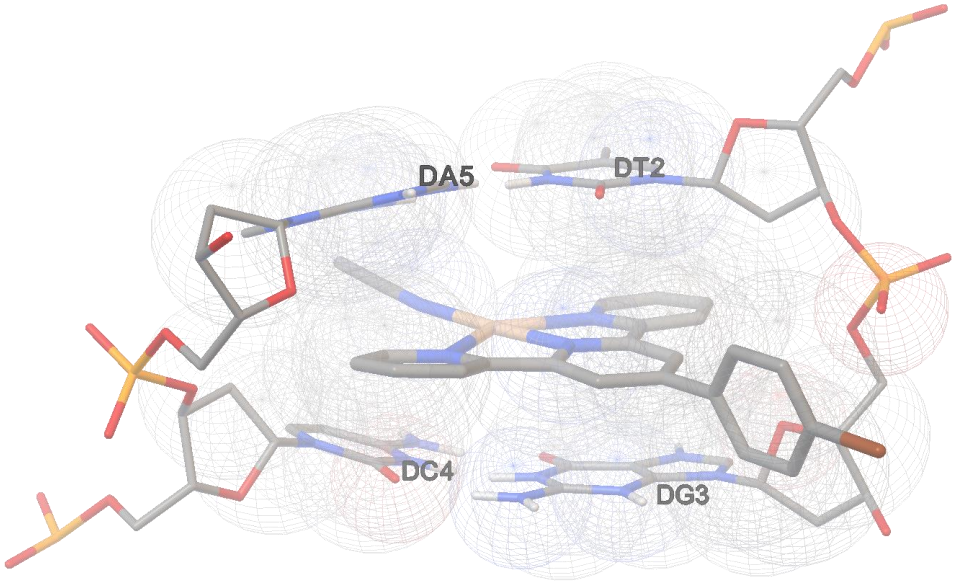

Figure S57 The most favorable orientation of compound **5** intercalating with the DNA (4JD8).

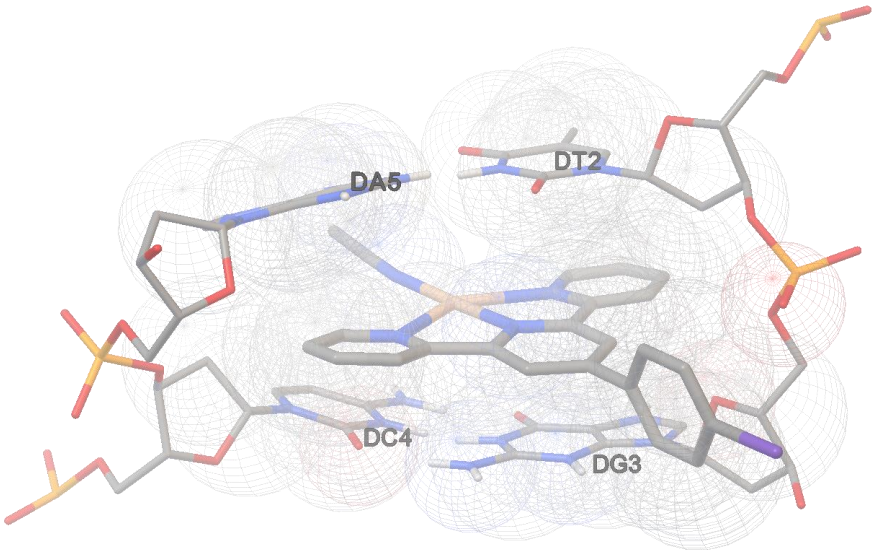

Figure S58 The most favorable orientation of compound **6** intercalating with the DNA (4JD8).

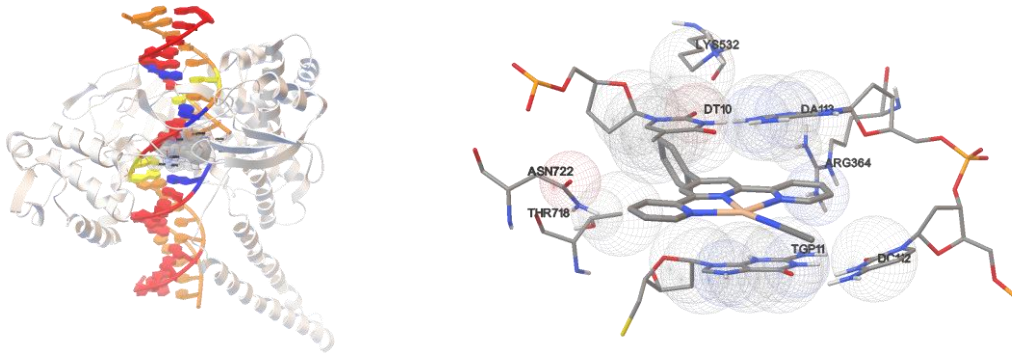

Figure S59 Molecular docking models of **1** in the active site of DNA–Topo I complex (PDB ID: 1T8I).

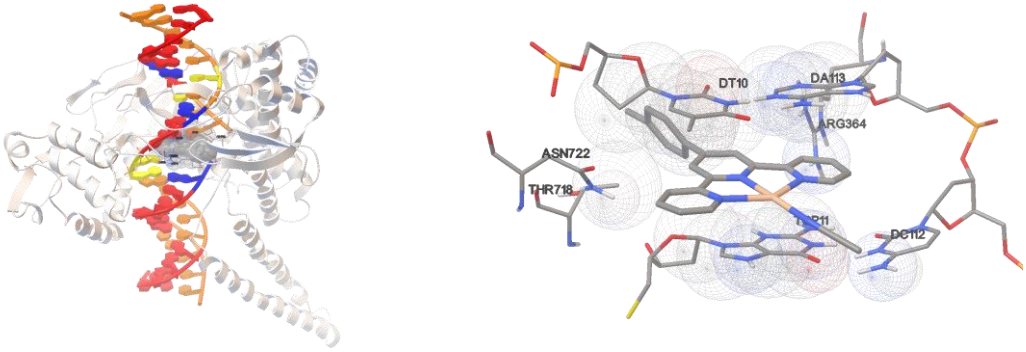

Figure S60 Molecular docking models of **2** in the active site of DNA–Topo I complex (PDB ID: 1T8I).

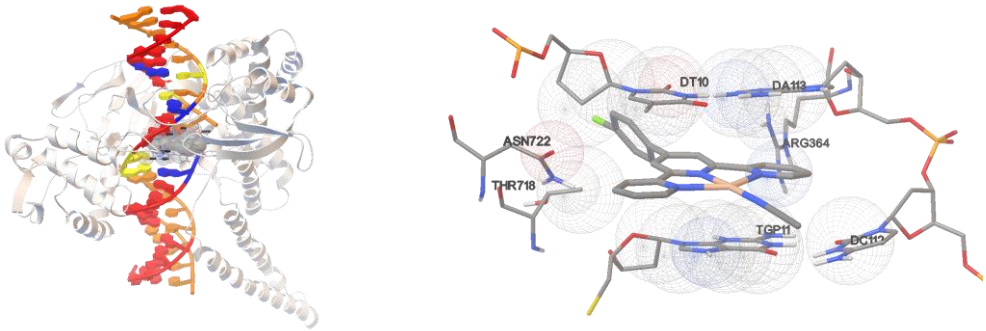

Figure S61 Molecular docking models of **4** in the active site of DNA–Topo I complex (PDB ID: 1T8I).

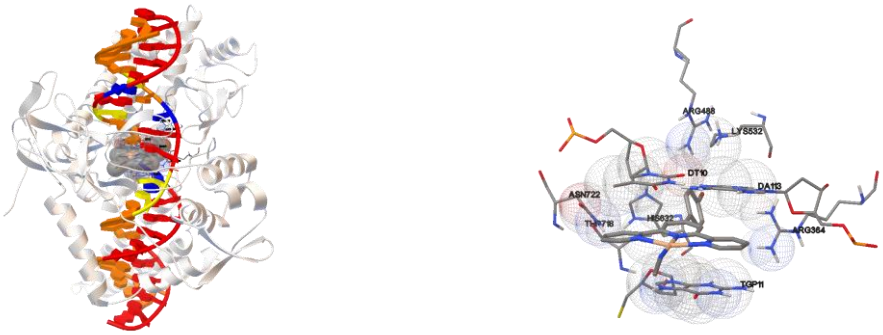

Figure S62 Molecular docking models of **5** in the active site of DNA–Topo I complex (PDB ID: 1T8I).

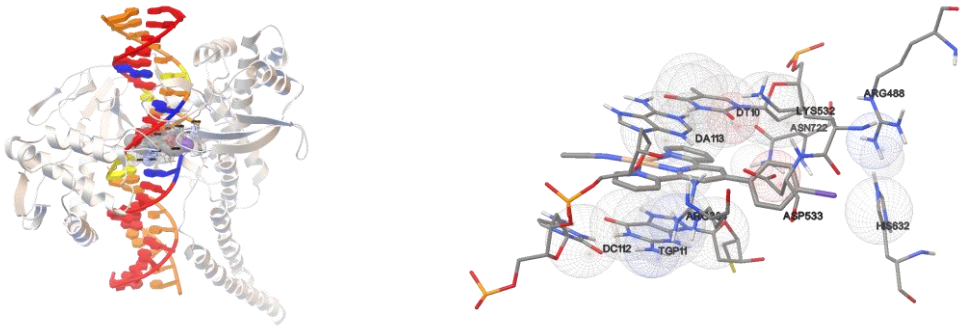

Figure S63 Molecular docking models of **6** in the active site of DNA–Topo I complex (PDB ID: 1T8I).